


 Cite this: *RSC Adv.*, 2025, 15, 39498

# Valorization of *Channa striatus* waste skin for developing marine collagen peptide based hydrogels for potential wound dressings

 Tanjina Tarannum, Farhana Islam, Khondoker Kabbyo Shariar and Nafisa Islam \*

This study focuses on the extraction and characterization of a bioactive collagen peptide from waste skin of a local species of fish, the *Channa striatus*/snakehead/'shol' fish. The extracted peptides were characterized and optimized for the formulation of chitosan/PVA/collagen peptide (CP) hydrogel which has not been done previously. The facile extraction process involved using alkali, butanol, and protease for non-collagenous protein and fat removal, and enzymatic hydrolysis respectively. Hydrogels were formulated using a non-toxic freeze-thaw technique with multiple combinations of chitosan, PVA, and collagen peptide and characterized with SEM, FTIR, swelling ratio, gel content, porosity, evaporation rate, and antibacterial and anti-inflammatory activity. The FTIR fingerprint of the collagen peptide confirmed the presence of characteristic amide bonds. The SEM image of the collagen peptide reveals an open morphological structure suggesting that enzymatic hydrolysis could produce lower molecular weight collagen peptide. The collagen peptide retained 53.31% total protein in which essential amino acids – 27.3% glycine, 8.74% arginine, and 14.11% proline – were present. Antioxidant properties – DPPH, hydroxide, and superoxide radical scavenging activity – demonstrated a linear correlation with collagen peptide concentration. The swelling ratio, a crucial structural property for a hydrogel, was the highest (619%) for Ch/PVA<sub>5</sub>-CP<sub>2</sub> (Chitosan: PVA: Collagen peptide = 1: 5: 2). The chitosan and collagen peptide served as key bioactives to facilitate wound healing, and PVA reinforced the bionanocomposite. The Ch/PVA<sub>5</sub>-CP<sub>2</sub> hydrogel had multiple bioactive properties and antibacterial activity against Gram-positive bacteria *S. aureus* and Gram-negative bacteria *E. coli*, anti-inflammatory activity, antioxidant activity and well-balanced mechanical stability and elasticity. In a preliminary seven-day trial on mice, this formulation showed promising results in treating burn wounds compared to commercial burn ointment (silver sulfadiazine 1%), and a negative control, warranting further *in vivo* studies using the hydrogel.

 Received 5th August 2025  
 Accepted 7th October 2025

DOI: 10.1039/d5ra05717e

[rsc.li/rsc-advances](http://rsc.li/rsc-advances)

## 1 Introduction

The socio-economic burden associated with frequently occurring non-healing wounds has been challenging society throughout the world. The early and late complications related to wound healing cause damage, morbidity, and mortality.<sup>1,2</sup> Many topical treatments are available worldwide to accelerate dermal wound healing. But often the problem lies in the mode of delivery, not the therapeutic element. Applying therapeutic agents directly to the wound is beneficial because of the direct benefits while limiting the side effects. Nevertheless, the proteolytic wound microenvironment and multiple underlying health conditions decrease the efficacy and bioavailability of the drug.<sup>3</sup> Many active therapies are available for burn wound treatment. Still, their key drawbacks lie in poor efficacy on deep wounds, visible scar formation, and high cost when used for prolonged periods.<sup>4,5</sup> The burn wound closure rate in a moist

condition theoretically doubles compared to a dry state and the moist dressing reduces the pain at rest, during movement, and dressing change<sup>6</sup> decreasing the tension in the wound. Hence, scientists are focused on developing alternative modern wound dressings. Modern dressing like hydrogels, films, and foams, offers multiple advantages that include creating a moist breathable environment, absorbing exudates, reducing side effects, protecting the area, accelerating the dermal restoration, and overcoming the proteolytic environment.<sup>7</sup>

Hydrogels are gel-like water-insoluble polymeric scaffolds that swell in the presence of water due to extensive cross-linking and the presence of functional groups (*i.e.*, amino, carboxyl, amide, hydroxyl, and sulphonic).<sup>8</sup> Tailorable functionality and release profile make hydrogels more attractive for targeted wound healing applications.<sup>9</sup> Collagen, cellulose, chitin, gelatin, and chitosan are some natural polymers, which when synthesized into a hydrogel show excellent biocompatibility. Inherent hemostatic, biodegradability, antibacterial properties, and broad-spectrum wound healing properties make the hydrogels an ideal candidate for developing hydrogel wound

Department of Chemical Engineering, Bangladesh University of Engineering and Technology, Dhaka 1000, Bangladesh. E-mail: [nafisaislam@che.buet.ac.bd](mailto:nafisaislam@che.buet.ac.bd)



dressings.<sup>10</sup> Chitosan can potentially participate in all phases of the wound healing process, starting from blood clotting, the aiding of neutrophil and macrophage migration<sup>11,12</sup> to cleaning the wound, and the formation of granulation and fibrous tissue.<sup>13</sup> In the remodeling stage, chitosan can reduce visible scar formation and allow slow re-epithelialization.<sup>7</sup> However, pristine chitosan-based hydrogels have poor mechanical properties.<sup>14</sup> Synthetic, biocompatible, and non-toxic polymers, such as polyvinyl alcohol (PVA) can provide desired reinforcement to chitosan-based hydrogels. Furthermore, the ability of PVA to create a physically crosslinked hydrogel network through a simple, non-toxic (no chemical cross-linker), and inexpensive freeze-thawing method enhances its appeal for tissue engineering applications.<sup>15</sup> Due to their enhanced mechanical properties, chitosan-PVA hydrogels have thus been used for biomedical applications including wound healing.<sup>16</sup>

With advances in biotechnology, the incorporation of biologically active compounds into wound healing scaffolds or hydrogels has been studied. Materials such as collagen, hyaluronic acid, vitamins, peptides, nanoparticles, and even cells and cytokines can be incorporated into hydrogels to facilitate wound healing by maintaining moisture, providing structural support, and promoting tissue regeneration,<sup>17</sup> protecting against infection,<sup>18</sup> reducing oxidative stress and inflammation,<sup>19</sup> accelerating cellular activity and tissue repair,<sup>20</sup> stimulating cell proliferation, angiogenesis, and tissue regeneration.<sup>21</sup> Mammalian collagen, specifically porcine, and bovine, served as an inexpensive source of collagen for a long time. The recent outbreaks of Foot and Mouth disease, Animal Prion disease, and religious conflicts associated with the consumption of such collagen have deterred the use of these products. Hence, in the search for alternative sources of collagen, marine collagen has drawn the attention of many researchers.<sup>22</sup> There are some commercially available collagen-based dressings such as Alloderm™ (human dermis), Amniograph™ (amniotic membrane), Oasis™ (porcine skin), Biobrane® (porcine collagen). On the other hand, marine collagen peptides can be sourced from fish byproducts such as scales and skin, and the most suitable method for peptide extraction is enzymatic hydrolysis.<sup>23</sup> These marine collagen peptides have superior properties to collagen including low molecular weight, stronger water affinity, easier absorption,<sup>24</sup> and most importantly heat stability at body temperature.<sup>25</sup> Moreover, collagen peptides have anti-aging, antioxidant, anti-hypertensive, anti-microbial, and wound-healing properties when administered orally, systematically, or topically.<sup>26,27</sup> Several studies have reported formulations with chitosan/PVA/nanoparticle,<sup>18,28</sup> chitosan/marine peptide,<sup>29</sup> and chitosan/PVA/collagen<sup>30</sup> hydrogels. Recently, scientists have focused on the wound-healing potential of hydrogels made from gelatin, collagen, or collagen peptides derived from tilapia skin. These materials have been formulated into biocomposites either independently<sup>31</sup> or combined with other substances like chitosan,<sup>31</sup> hyaluronic acid,<sup>32</sup> adipose-derived stromal vascular fraction,<sup>33</sup> and nano-hydroxyapatite/chitosan<sup>34</sup> to boost the healing performance. Sun *et al.* (2022) prepared a sea bass scale gelatin/kelp sodium alginate/chitosan-based nanofiber hydrogel

infused with copper sulfide nanoparticles to explore *in vivo* wound healing efficacy.<sup>35</sup> Snakehead fish, *Channa striatus*, locally known as 'shol' and abundantly found in South Asia, is recognized for its therapeutic and nutritional benefits owing to its high protein content (17% w/w collagen). This fish enriched with high amino and fatty acid content, is potent for accelerating post-operative wound healing.<sup>36</sup> To the best of our knowledge, no study has yet reported the chemical characterization or application of collagen peptides, derived from snakehead fish waste, nor the synthesis, structural, and bioactive properties of extracted marine collagen peptide-based chitosan/PVA hydrogel. This study, therefore, aims to investigate the characteristics of collagen peptide derived from locally sourced fish waste, exploring its potential as an alternative source of collagen peptide additive for PVA-chitosan hydrogel for wound healing applications.

## 2 Methodology

### 2.1 Materials

Polyvinyl acetate (PVA)  $[-CH_2CHOH-]_n$  (MW: 125 000 g mol<sup>-1</sup>) was purchased from PT. Smart Lab, Indonesia. Chitosan (LMW, extra pure, 90% deacetylated degree), tris buffer (>99.9%), and Bradford reagent were obtained from Sisco Research Laboratories Pvt Ltd, India. Methanol (>99.5%), pyrogallol, and salicylic acid, albumin bovine fraction V (>98%, MW: 66.5 kDa) were purchased from Research-lab Fine Chemical Industries, India. Protamex® (protease from *Bacillus* sp. and DPPH were purchased from Sigma-Aldrich. Absolute Ethyl Alcohol (>99.9%) was purchased from BRG Biomedicals, India. Acetic acid (glacial, ≥ 99%), sodium chloride, potassium chloride, potassium dihydrogen phosphate, disodium hydrogen phosphate dihydrate, iron(II) sulfate heptahydrate (≥98.5%), sodium hydroxide (≥98%) were all purchased from Merck Life Science Pvt Ltd, India. Hydrochloric acid was purchased from RCI Labscan Ltd Mueller-Hinton, and MacConkey agar and broth were purchased from Himedia, India. *n*-butanol (>99%) was procured from Daejung Chemicals. All reagents and chemicals were of analytical grade and used as is.

### 2.2 Collagen peptide extraction and characterization

**2.2.1 Collagen peptide extraction.** The fish skin waste, collected from Palashi Market (local market), was cleaned to remove debris. The skin was pretreated first according to Arumugam *et al.* (2018).<sup>37</sup> Non-collagenous proteins were removed by 0.3 M NaOH at 1/10 (w/v) with continuous stirring for 4 h while replacing the NaOH solution every hour. The collected skins were repeatedly washed with distilled water to reach a neutral pH. Then the skin was defatted with 20% (v/v) butanol for 30 h for 10 ml butanol/gm skin. The butanol solution was replaced every 10 h. The skin was neutralized by repeated washing with distilled water followed by homogenization. After pretreatment, the homogenized skin was subjected to enzymatic hydrolysis for collagen peptide extraction according to Ennaas *et al.* (2015).<sup>38</sup> The homogenized sample was heated to 50 °C and Protamex® enzyme was added at 0.15% (w/w) of the



raw material. The pH was maintained at near neutral before the hydrolysis commenced. No pH regulation was followed during the hydrolysis time. After 6 hours, the mixture was heated at 90 °C for 10 min to stop the hydrolysis and centrifuged at 20000×g for 30 min at 4 °C. The supernatant was filtered with Whatman 40 filter paper followed by a nylon (PA) 0.45 μm syringe filter. Finally, the filtrate was freeze-dried and stored at −20 °C.

**2.2.2 Protein content.** According to Marion M. Bradford,<sup>39</sup> a standard curve of bovine serum albumin (BSA) concentrations was generated in the range of 100–1000 μg ml<sup>−1</sup>. Initially, 50 μl solution of the BSA (standard) or collagen peptide (sample) was mixed with 2500 μl of Bradford reagent and allowed to react for 15 min. The absorbance of the solutions was measured at 595 nm. The protein content of the extracted peptide was determined from the standard curve of BSA. The reference contained distilled water instead of the protein.

**2.2.3 Amino acid composition.** 0.3 g of collagen peptide was digested overnight at 102 °C with 3 : 1 (water : HCl) acid and 0.1 mg phenol mixture. The mixture pH was adjusted (pH 2) with NaOH, diluted to 100 mL, and filtered with a 0.22 μm syringe filter. For sample, standard dilution and for the mobile phase citrate buffers were prepared as provided by the manufacturer. The amino acid composition was analyzed by 1 h runtime with an amino acid analyzer (S 433-D, Sykam GmbH, Germany). The analyzer specifications were column: LCA K07/Li (PEEK – column 4.6 × 150 mm), detector: photometer (570 nm, 440 nm), detection principle: ninhydrin reaction.

**2.2.4 DPPH free-radical scavenging assay.** Briefly, 0.5 mL collagen peptide solution (1–8 mg mL<sup>−1</sup>) was mixed with 2.0 mL, 0.1 mM DPPH in methanol, and left in the dark to react for 30 min at room temperature.<sup>40</sup> The absorbance was measured at 517 nm. The scavenging effect of DPPH radical was evaluated using the following equation.

$$\text{Scavenging activity(\%)} = \frac{A_{\text{control}} - A_{\text{sample}}}{A_{\text{control}}} \times 100\% \quad (1)$$

Here,  $A_{\text{control}}$  and  $A_{\text{sample}}$  represent the absorbance of the negative control and sample respectively.

**2.2.5 Superoxide anion radical scavenging assay.** Briefly, 0.2 mL collagen peptide solution (1–8 mg mL<sup>−1</sup>) was mixed with 4 mL distilled water and 4.5 mL 50 mM Tris–HCl buffer (pH 8.2) and incubated at 25 °C for 10 min. Then 0.3 mL 3 mM pyrogallol solution (HCl as solvent) was added to the mixture and the absorbance was immediately measured at 320 nm with 30 s intervals for 5 min.<sup>40</sup> Distilled water was used as a negative control. The superoxide anion radical scavenging activity was calculated using the following equation.

$$\text{Scavenging activity(\%)} = \frac{S_{\text{control}} - S_{\text{sample}}}{S_{\text{control}}} \times 100\% \quad (2)$$

where  $S_{\text{control}}$  and  $S_{\text{sample}}$  represent the slopes of absorbances of the control and sample respectively.

**2.2.6 Hydroxyl radical scavenging activity assay.** Briefly, 1 mL collagen peptide solution (1–8 mg mL<sup>−1</sup>) was mixed with 8 mM 0.3 mL of FeSO<sub>4</sub>·7H<sub>2</sub>O, 3 mM 1 mL of salicylic acid in ethanol, and 20 mM 0.25 mL of H<sub>2</sub>O<sub>2</sub> solutions. The mixture was incubated at 37 °C for 30 min. Finally, distilled water was

added to make a final volume of 3 mL. The mixture was centrifuged at 3000×g for 10 min and the absorbance of the supernatant was measured at 510 nm. Distilled water was used as a negative control.<sup>40</sup> The scavenging activity of the hydroxyl radical was calculated according to eqn (1).

## 2.3 Hydrogel preparation and characterization

**2.3.1 Hydrogel preparation.** The physically crosslinked chitosan/PVA-collagen peptide hydrogels were prepared by the freeze-thaw technique, modified from Figueroa-Pizano *et al.* (2019)<sup>41</sup> and following the protocol from Islam *et al.* (2024).<sup>42</sup> First, the hydrogel precursor solutions of 2% (w/v) chitosan and 10% (w/v) PVA solutions were prepared. 2% (w/v) chitosan solution was prepared in 0.1 M acetic acid with overnight stirring at room temperature. 10% (w/v) PVA was prepared in distilled water at 80 °C with 4 hours of stirring and cooled down before further use. Then chitosan and PVA were mixed at the desired ratio with 5 minutes of stirring. Collagen peptide was added at the proper ratio to chitosan with 2 hours of stirring, followed by 10 minutes of sonication to remove air bubbles and get a homogenous solution. A cylindrical plastic container was used as the hydrogel mold. The freeze-thaw cycle was initiated by keeping the solution at −20 °C for 12 hours to freeze and at 25 °C for 4 hours to thaw, which completed one cycle and thus continued for four more cycles. After five complete cycles, all the hydrogels were soaked in distilled water until neutral pH to remove the excess acetic acid, the unbonded polymer molecules, and ions from the hydrogel. The hydrogels were freeze-dried and stored in a desiccator until further analysis. Six hydrogel combinations were prepared by altering two factors — the chitosan: PVA weight ratio (at 1 : 5 and 1 : 10); and the chitosan to collagen peptide weight ratio (at 1 : 0, 1 : 1, and 1 : 2). In this article, chitosan/PVA-collagen peptide hydrogels are denoted by Ch/PVA<sub>x</sub>-CP<sub>y</sub>, where  $x$  represents the weight ratio of PVA to chitosan (Ch), and  $y$  specifies the weight ratio of collagen peptide (CP) to chitosan. For instance, a sample identified as Ch/PVA<sub>5</sub>-CP<sub>1</sub> represents a hydrogel with a chitosan and PVA weight ratio of 1 : 5 and a chitosan and collagen peptide weight ratio of 1 : 1. All hydrogels having chitosan: PVA ratio 1 : 5 are referred to as Ch/PVA<sub>5</sub> hydrogels, and the hydrogels having chitosan: PVA ratio 1 : 10 are referred to as Ch/PVA<sub>10</sub> hydrogels.

**2.3.2 Porosity.** The porosity of the freeze-dried hydrogel was measured according to Kalantari *et al.* (2020) using the following equation.<sup>18</sup>

$$\text{Porosity(\%)} = \frac{W_w - W_d}{W_w - W_i} \times 100 \quad (3)$$

Here,  $W_d$ ,  $W_i$ , and  $W_w$  represent the weights of dry hydrogel, hydrogel immersed in ethanol, and hydrogel taken out of ethanol respectively.

**2.3.3 Swelling ratio and gel content.** The freeze-dried hydrogel of thickness 5 mm thickness (diameter 10 mm) was weighed ( $W_d$ ) and soaked in 10 mL phosphate-buffered saline (pH 7.4) at 37 °C. After 24 h, gels were taken out, wiped on the filter paper, and weighed ( $W_s$ ). Then the swollen hydrogels were dried at 50 °C for 48 hours until constant weight ( $W_c$ ). The



swelling ratio and gel content were calculated using the following equations.

$$\text{Swelling ratio(\%)} = \frac{(W_s - W_d)}{W_d} \times 100 \quad (4)$$

$$\text{Gel content(\%)} = \frac{W_c}{W_d} \times 100 \quad (5)$$

**2.3.4 Water evaporation rate.** To measure the water evaporation rate, the swollen hydrogels (10 mm diameter and 7.5 mm thickness) were kept at 37 °C, 40% humidity, and weighed at regular intervals until constant weight.<sup>43</sup> The water loss was determined with the following equation.

$$\text{Evaporation rate(\%)} = \frac{W_s - W_t}{W_s - W_f} \times 100 \quad (6)$$

Here,  $W_s$ ,  $W_t$  and  $W_f$  represent the initial weight, measured weight at different times, and final constant weight, respectively.

**2.3.5 FTIR.** The freeze-dried samples (collagen peptide, PVA, chitosan, hydrogel) were scanned between 500 and 4000  $\text{cm}^{-1}$  wavenumbers using ATR-FTIR (Nicolet™ iS5 FTIR Spectrometer, ThermoFisher Scientific, WI, USA) to understand the interaction of functional groups and polymer bonds in the scaffold.

**2.3.6 Scanning electron microscopy (SEM) imaging.** The morphology of hydrogel and collagen peptide were analyzed with SEM (EVO 18, Zeiss, Germany). The sample was coated with gold sputtering using a mini sputter coater/glow discharge system first and then the structure was imaged with SEM at 15 and 10 kV the accelerating voltage.

**2.3.7 Mechanical properties of hydrogel.** The compressive mechanical properties of hydrogels (10 mm diameter, 10 mm thick) were measured with a universal testing machine (100P250-12, TestResources, USA). The swollen hydrogel was subjected to a 10 N load cell at a rate of 10  $\text{mm min}^{-1}$ .

**2.3.8 Anti-inflammatory study.** The anti-inflammatory study of the hydrogel is an indirect measure that tests the hydrogel's ability to inhibit protein denaturation at body temperature; bovine serum albumin (BSA) was used as a model protein for this purpose. According to Ruffo *et al.* (2022), 0.1 g of hydrogel was immersed in 2 ml, 1 mM BSA dissolved in phosphate-buffered saline (pH 7.4). The solution was incubated for 30 min to initiate BSA denaturation and the absorbance was noted at 660 nm in UV-vis spectrophotometer.<sup>44</sup> The inhibition of BSA denaturation was estimated using eqn (5).

$$\text{Inhibition(\%)} = \frac{A_1 - A_0}{A_0} \times 100 \quad (7)$$

Here  $A_0$  and  $A_1$  are the absorbance at 660 nm, after 30 minutes of incubation with the control and sample, respectively.

**2.3.9 Antibacterial study.** The antibacterial activity of the hydrogels was tested against *S. aureus* ATCC653 (Gram-positive) and wild-type *E. coli* 0157:H7 (Gram-negative) using a modified Kirby–Bauer disk diffusion method. Muller–Hinton broth and agar (Himedia) were used as culture media. Hydrogels were

sliced (5 mm thickness, 10 mm diameter) and washed with distilled water. Then the gels were sterilized in a UV chamber for 30 min followed by rehydration with sterile distilled water for the next 30 min. Bacteria from overnight liquid culture were diluted in the range of McFarland standard OD600 = 0.1 ( $\sim 10^8$  CFU  $\text{mL}^{-1}$ ). Afterward, the diluted bacteria were inoculated uniformly on an agar surface with sterile cotton swabs. The agar surface was dried before placing rehydrated hydrogels on the agar surface and leaving them in the incubator overnight at 37 °C. The inhibition zone was measured by using a scale.

## 2.4 Statistical analysis

Tests were performed in triplicate and GraphPad Prism software was used for data visualization and statistical analysis. Error bars were obtained as the mean  $\pm$  standard deviation (SD). A two-way ANOVA test was done to check the significance between results with significance specified as \* $p < 0.05$ , \*\* $p < 0.01$ , and \*\*\* $p < 0.001$ ,  $n = 3$ .

## 2.5 Preliminary *in vivo* wound healing evaluation

**2.5.1 Animals and experimental method.** The animal trial was performed in compliance with the NIH guidelines (2011) for the care and use of laboratory animals and has been approved by the Ethics Committee of Department of Chemical Engineering, Bangladesh University of Engineering and Technology.<sup>45</sup> The preliminary experiment has been designed to corroborate with ARRIVE (Animal Research: Reporting of *In Vivo* Experiments) guidelines. As a preliminary *in vivo* healing study, nine albino mice (female, 6 to 8 weeks old, weight 20–30 g) were used. Animals were separately kept in clean polyethylene cages under usual experimental conditions of temperature  $25 \pm 2$  °C and fed *ad libitum*. Three groups of mice were chosen randomly—one group received the (Ch/PVA<sub>5</sub>-CP<sub>2</sub>) hydrogel, the second group was the positive control group and received local burn ointment, silver sulfadiazine 1%, and the final group was the negative control receiving no treatment. In each group, two mice were tested for wound healing for 7 days and the third mouse, for 14 days. All animals were anesthetized with Ketamine HCl (100  $\text{mg mL}^{-1}$ ), shaved, and sterilized with 70% ethanol. The burn wounds were induced by a 10 mm (diameter) metal rod. The metal rod was heated with a Bunsen burner for 20 seconds and placed on the shaved dorsum for 5s to create the partial-thickness burn wound. This was followed by applying either the test hydrogels or the positive control ointment, according to the treatment scheme. The treatments were reapplied every two days, after cleaning with sterile saline. The wound was photographed with a ruler placed at the bottom for scale. The animals were sacrificed after the completion of the experimental period.

**2.5.2 Measurement of wound area.** The changes in burn area were measured using ImageJ software from the photographs. Burn wound healing was expressed as the decrease in the original burn area percentage. The detailed results have been discussed in the Supplementary Information Document (SI).



### 3 Results and discussion

#### 3.1 Protein content, amino acid profile, and antioxidant activity of collagen peptide

The waste skin of snakehead fish, *C. striatus*, was locally sourced from Palashi Market and used as raw material to extract collagen peptide. The final extract was positively identified as collagen peptide with a simple water solubility test because, unlike collagen, collagen peptide is highly soluble in water at room temperature.<sup>46</sup> Moreover, under the experimental conditions of high temperature, basic treatment, and enzymatic hydrolysis as described in the methods, it is unlikely that the final extract will retain any collagen or gelatin. The product was subject to further characterization and used as a component of hydrogels, as described in the following sections.

**3.1.1 Collagen peptide characterization.** Extracted collagen peptide (CP) was slightly yellowish, milky-colored granules (shown in Fig. 1a) that when viewed under a scanning electron microscope (SEM) revealed open pores on the surface, as represented in Fig. 1b. The irregular pores in the collagen peptide likely resulted from the degradation of the collagen fibrils assembly due to enzymatic action leading to low molecular weight collagen peptide.<sup>47</sup> Chi *et al.* (2014) extracted collagen hydrolysate from Spanish mackerel skin and observed that lower molecular weight collagen peptides had a more open and porous structure.<sup>48</sup> Bradford assay revealed that the total amount of protein in the extracted peptide from snakehead fish was  $53.31 \pm 1.26\%$ . That is consistent with the protein content in mackerel and its by-product hydrolysates with 69.23% and 52.43% protein respectively with Protamex-driven hydrolysis under different hydrolysis conditions.<sup>38</sup> However, the total protein content does not account for free arginine or lysine, or polypeptide chains shorter than 3000 Da in the collagen peptide, a limitation of Bradford assay dye.<sup>49–51</sup> The extracted peptide was compared with a sample of commercially produced marine collagen peptide powder (Type I) extracted from wild-caught, deep-sea fish (purchased from Correxiko, USA). The details of the comparison of the extracted and commercially obtained peptide are provided in SI Section S1. The extracted peptides showed chemical similarities with the commercial peptide and thus the extracted peptides are expected to show

the physio-chemical properties of peptides that are commercially extracted from marine sources.

**3.1.2 Amino acid profile.** Amino acid analysis of the extracted collagen peptide (CP) from *C. striatus* is presented in Table 1. The extracted CP contains 27.3% glycine, 8.74% arginine, and 14.11% proline, exceeding the corresponding amino acid levels of collagen peptide extracted from tilapia – 20.4% glycine, 7.9% arginine, and 10.8% proline.<sup>29</sup> Glycine takes part in many important biochemical reactions, including the production of DNA, proteins, and heme, lipid metabolism, immune regulation, and neurotransmission. Good biocompatibility, biodegradability, and excellent mechanical properties along with the potential to improve immunity and inflammation, wound healing, and even neurological function make it suitable for biomedical applications.<sup>52</sup> Arginine is a proline precursor. Proline is essential for the synthesis of collagen and can promote the production of biologically active molecules in the body.<sup>52</sup> While a particular amino acid can trigger a particular healing pathway, a blend of amino acids can activate multiple simultaneous pathways to heal a wound. Liu *et al.* (2018) reported that among 20 amino acids, nine showed antioxidant activity, and their mixtures demonstrated synergistic effects.<sup>53</sup> Interestingly, some amino acids, like tyrosine, methionine, histidine, lysine, and tryptophan, are inherently antioxidant and exhibit even higher antioxidant activity when incorporated into peptides.<sup>54</sup> Hence, delivering an amino acid blend in the form of a peptide to the wound is more effective

Table 1 Amino acid profile of CP

Amino acid	Amount (%)	Amino acid	Amount (%)
Glycine	27.30	Cystine	0.38
Alanine	14.79	Methionine	1.54
Proline	14.11	Isoleucine	0.50
Glutamic acid	11.51	Leucine	1.49
Arginine	8.74	Tyrosine	0.43
Aspartic acid	5.23	Phenylalanine	1.80
Serine	3.86	Histidine	0.61
Lysine	3.21		
Valine	2.04		
Threonine	2.46		

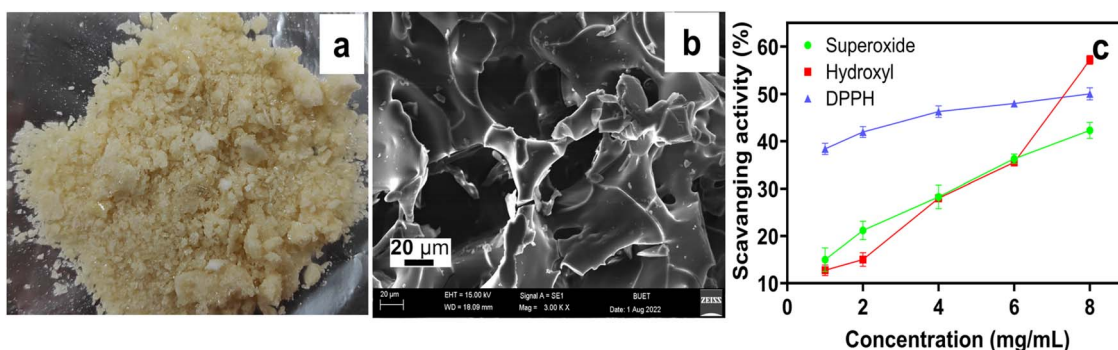


Fig. 1 (a) Physical image of extracted collagen peptide, (b) SEM of freeze-dried collagen peptide, and (c) antioxidant activity (ordinate) of collagen peptide against superoxide, hydroxyl, showing DPPH free radical increases with higher collagen peptide concentrations (abscissa).



than as a protein or individual amino acids because peptides can easily break down into smaller peptides or amino acid blends with potentially superior antioxidant properties in the proteolytic wound environment.

### 3.1.3 Antioxidant properties of the collagen peptide.

Immune cells can fight against microorganisms by producing reactive oxygen species (ROS), which is the predominant cause of the inflammatory phase in chronic wounds. In chronic wounds, the situation can take a turn for the worse by ROS overproduction and inflicting damage to cells and extracellular matrix,<sup>55</sup> eventually delaying the healing process. Existing literature suggests that the antioxidant properties of potential wound-healing compounds are closely related to deactivating the produced ROS by scavenging free radicals, chelating transition metals, and donating electrons or hydrogen.<sup>48</sup> The estimation of the scavenging activity of free radicals provides an indirect measure of the antioxidant property of the compound. DPPH assay is widely used to investigate an antioxidant's stable radical scavenging activity. Although superoxide anion radical is not a strong oxidant and is not usually evaluated to investigate the antioxidant properties, it is the potential precursor to other stronger and more damaging ROS like hydroxyl radical. Therefore, removal or entrapment of hydroxyl radical or its potential precursor is very important.<sup>40</sup> In our study, the radical scavenging activity of collagen peptide was assessed by DPPH, hydroxyl, and superoxide radical scavenging assays. As illustrated in Fig. 1c, DPPH, superoxide, and hydroxyl radical scavenging activity increased linearly within CP concentrations ranging from 1–8 mg mL<sup>-1</sup> and the strongest scavenging action resulted in the highest CP concentration (8 mg mL<sup>-1</sup>).

The highest scavenging action by collagen peptide against DPPH, OH, and superoxide radicals were 50%, 57.17%, and 42.3% respectively. Another study of snakehead flesh hydrolysate reported DPPH scavenging activity ranging from 13.25%–22.47% where hydrolysis conditions and procedure were

different from this study.<sup>56</sup> DPPH scavenging activity of Spanish mackerel collagen hydrolysate ranged from 35.82–65.72% and the hydroxyl scavenging activity ranged from 41.27–76.99%.<sup>48</sup> Therefore, the antioxidant property of the extracted peptide can be ascribed to its ability to scavenge the superoxide, hydroxyl, and DPPH free radicals.

## 3.2 Hydrogel characterization

The collagen peptide extracted from snakehead fish skin were incorporated into chitosan/PVA hydrogels and their properties were evaluated to assess their potential as wound healing material. Chitosan/PVA-collagen peptide hydrogels are denoted by Ch/PVA<sub>x</sub>-CP<sub>y</sub>, where *x* represents the weight ratio of PVA to chitosan (Ch), and *y* specifies the weight ratio of collagen peptide (CP) to chitosan.

**3.2.1 FTIR spectroscopy of hydrogels.** FTIR spectra of the components and the final hydrogel were observed to confirm the crosslinking within the chitosan/PVA hydrogels incorporating extracted collagen peptide. As illustrated in Fig. 2a, the FTIR spectra of PVA represented the characteristic peaks at 3290 cm<sup>-1</sup> for –OH stretching, 2920 cm<sup>-1</sup> for –CH<sub>2</sub>-asymmetric stretching, 1420 and 1090 cm<sup>-1</sup> for C–O groups, and 833 cm<sup>-1</sup> for C–C stretching vibrations. For extracted peptide, the peaks at 3270 cm<sup>-1</sup> and 3080 cm<sup>-1</sup> represented amide A and B bands, and 1630, 1520, and 1240 cm<sup>-1</sup> represented the amide I, II, and III bands of polypeptide chains respectively. The peak at 2930, 1450, and 1390 cm<sup>-1</sup> corresponds to the C–H stretching vibrations, and C–H and O–H bending vibrations respectively.<sup>57</sup> For chitosan, the peaks were at 1650 cm<sup>-1</sup> (C=O stretch), 1590 cm<sup>-1</sup> (–NH bend), 1370 cm<sup>-1</sup> (–CH bend), and 1020 cm<sup>-1</sup> (C–O stretch) on the spectra.<sup>58</sup> The broadband signal between 3200–3450 cm<sup>-1</sup> in the hydrogel shifted and narrowed compared to pure PVA, pure collagen peptide, and chitosan spectra, indicating possible electrostatic interaction between

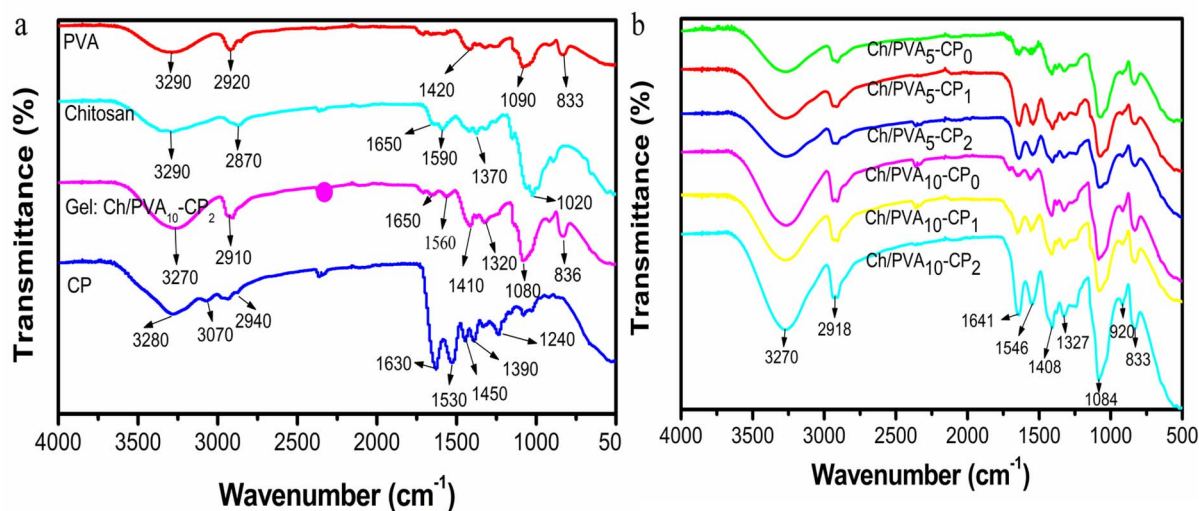


Fig. 2 (a) FTIR comparative spectra of PVA, chitosan, (Ch/PVA<sub>10</sub>-CP<sub>5</sub>) hydrogel, and collagen peptide (CP). Overlapping peaks from PVA, chitosan, and collagen peptide can be observed in the hydrogel spectrum. (b) FTIR spectra of various combinations of chitosan/PVA/collagen peptide. The spectra showed almost similar characteristic peaks for all hydrogels except for Ch/PVA<sub>5</sub>-CP<sub>0</sub> and Ch/PVA<sub>10</sub>-CP<sub>0</sub> (no amide peaks).



negatively charged peptide and positively charged chitosan<sup>59</sup> complemented by hydrogen bonds between these three constituent biomolecules.

As illustrated in Fig. 2b, the characteristic peaks at  $3270\text{ cm}^{-1}$  ( $-\text{OH}$  stretching),  $650\text{ cm}^{-1}$  ( $\text{C}=\text{O}$  stretch),  $2910\text{ cm}^{-1}$  (asymmetric  $-\text{CH}_2$ -stretching), and  $836\text{ cm}^{-1}$  ( $\text{C}-\text{C}$  stretching) were still present in the hydrogel. The  $-\text{OH}$  stretching peak of PVA and chitosan at  $3290\text{ cm}^{-1}$  overlapped with the amide A band at  $3280\text{ cm}^{-1}$  of collagen peptide and increased the peak intensity of hydrogel at  $3270\text{ cm}^{-1}$ .  $\text{C}-\text{O}$  stretching vibration at  $1020\text{ cm}^{-1}$  of chitosan and  $1090\text{ cm}^{-1}$  of PVA overlapped and shifted to  $1080\text{ cm}^{-1}$  for hydrogel.  $-\text{NH}$  vibration peak of chitosan at  $1590\text{ cm}^{-1}$  and  $1530\text{ cm}^{-1}$  for extracted collagen peptide faced intervention and formed an intermittent peak at  $1560\text{ cm}^{-1}$  instead. Some additional peaks in the hydrogel were observed due to possible random overlapping and hydrogen bonds in the intermolecular attraction; non-covalent interactions can account for all slight shifts in the peaks. All hydrogels had similar characteristic peaks (Fig. 2b). Amide peaks are absent in the formulations with no collagen peptide (Ch/PVA<sub>5</sub>-CP<sub>0</sub>, Ch/PVA<sub>10</sub>-CP<sub>0</sub>).

**3.2.2 Hydrogel swelling ratio, gel content, porosity, and evaporation rate.** The chitosan and PVA have hydrophilic groups with high water affinity, but physical or chemical crosslinking between the polymers can significantly reduce the dissolution of these polymers. Hydrogels with physical or chemically bonded polymeric networks are prepared so that they can absorb water and swell, which mimics the physical properties of living tissue.<sup>60</sup> The swelling capacity of a hydrogel is inversely correlated to the degree of crosslinking and on the

other hand, better crosslinking assists the mechanical property of hydrogel.<sup>61</sup> Hence, it is necessary to strike a balance between these characteristics for optimal hydrogel formulation. As shown in Fig. 3a, collagen peptide inclusion and PVA variation impacted the swelling behavior of hydrogel and results showed an increase in swelling ratio with an increasing amount of collagen peptide which we hypothesize is caused by more hydrogen bonds between collagen peptide and water molecules owing to the presence of amino acids with large side chains<sup>62</sup> (like arginine, glutamic acid), hydroxy groups<sup>63</sup> (like serine, threonine), and positively charged residues<sup>64</sup> (like lysine, arginine). Another possible explanation is that the peptides can partially interfere with the intermolecular hydrogen bonding and electrostatic interactions between PVA and chitosan, thereby reducing effective crosslink density. This leads to a more loosely arranged polymer matrix, which allows greater water penetration and retention. The combined influence of these factors likely accounts for the progressive increase in swelling ratio observed with higher peptide loading. A higher swelling was observed in Ch/PVA<sub>5</sub> hydrogel formulations, as compared to Ch/PVA<sub>10</sub> hydrogels. This occurs because relatively higher chitosan ratios in the hydrogels (Ch/PVA<sub>5</sub> hydrogels) can improve the swelling across a wide range of pH. The hydrogel formulations contain chitosan as one major constituent and its ionizable functional groups like  $-\text{NH}_2$ , and  $-\text{CH}$  assist the swelling in both acidic and basic media.<sup>65</sup> In addition, increasing PVA concentration has two possible consequences on the swelling behavior (comparing Ch/PVA<sub>5</sub> and Ch/PVA<sub>10</sub> hydrogels). First, with the increase of PVA, the likelihood of crosslink formation also increases,<sup>66</sup> resulting in a reduction of

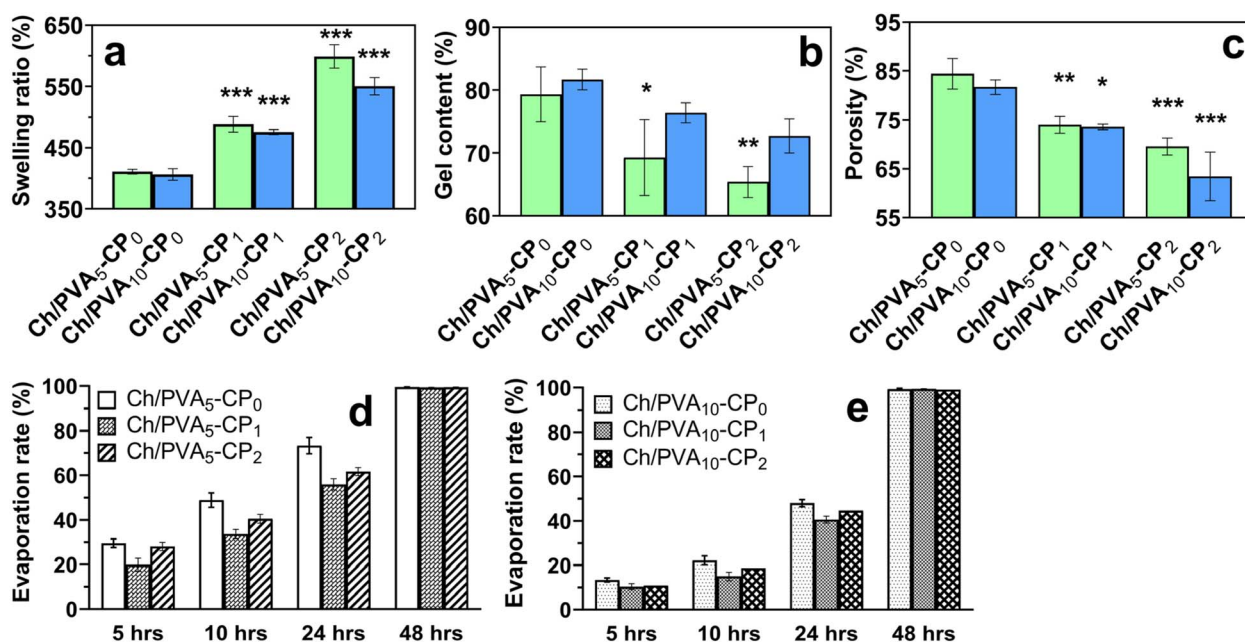


Fig. 3 Physical properties of hydrogels. (a) Swelling ratios -- highest swelling observed for Ch/PVA<sub>5</sub>-CP<sub>2</sub> and Ch/PVA<sub>10</sub>-CP<sub>2</sub> among all Ch/PVA<sub>5</sub> hydrogels and Ch/PVA<sub>10</sub> hydrogels respectively; (b) gel content -- lower for Ch/PVA<sub>5</sub> hydrogels; (c) porosity -- all hydrogels retained above 60% pores in the structure; (d) evaporation rates of Ch/PVA<sub>5</sub> hydrogel group, and (e) evaporation rates of Ch/PVA<sub>10</sub> = 1 : 5 combinations. Error bars represent the means standard error for  $n = 3$  and  $*p < 0.05$ ,  $**p < 0.01$ , and  $***p < 0.001$  with Ch/PVA<sub>5</sub>-CP<sub>0</sub> and Ch/PVA<sub>10</sub>-CP<sub>0</sub> as controls for corresponding groups.



the free hydroxyl groups in the polymer chain, slightly raising the hydrophobic nature of the hydrogel. Consequently, the number of free hydroxyl groups also decreases, decreasing the possibility to interact and bind with water molecules. Second, due to the higher crosslinking degree imparted by PVA, free space and chain mobility inside the network decrease. This restricts the water molecules from infiltrating, and binding, and ultimately causes lower swelling of the hydrogels. Ch/PVA<sub>5</sub>-CP<sub>2</sub> demonstrated the highest swelling capacity, reaching a maximum of 619%. A maximum of 644.2% swelling was observed for a PVA/Chitosan hydrogel in a study by Yang *et al.* (2018).<sup>66</sup>

Gel content in the hydrogel is a measure of the degree of cross-linking that is connected to and governs every other characteristic of the hydrogel. For wound dressing application of hydrogel, approximately 80% gel content is considered suitable,<sup>67</sup> and Ch/PVA<sub>5</sub>-CP<sub>0</sub>, Ch/PVA<sub>10</sub>-CP<sub>0</sub>, and Ch/PVA<sub>10</sub>-CP<sub>1</sub> approach this value. Within each group of Ch/PVA<sub>5</sub> or Ch/PVA<sub>10</sub>, gel content decreased with increasing concentration of collagen peptide that was likely caused by the degradation of collagen peptide during the network formation at higher ratios of collagen peptide. Collagen peptide degradation during network formation can arise from chemical modification, hydrolysis, or aggregation, and because such changes do not necessarily cause leaching, retention is difficult to evaluate. While monitoring peptide leaching may not fully capture degradation, it could provide an indirect indication of peptide loss; therefore, future work should focus on assessing peptide stability and retention more directly. Chemically modified hydrogels containing small molecules like small proteins can undergo gel degradation.<sup>68</sup> Furthermore, among the two hydrogel groups, Ch/PVA<sub>10</sub> hydrogels had relatively higher gel content than Ch/PVA<sub>5</sub> ( $p < 0.05$ ) (Fig. 3b). PVA polymerization is mostly governed by hydrogen bonds formed by the hydroxyl functional groups.<sup>69</sup> Higher gel content Ch/PVA<sub>10</sub> is influenced by stronger intramolecular hydrogen bonds due to additional hydroxyl groups. Although the gel content of Ch/PVA<sub>5</sub>-CP<sub>2</sub> gel content falls below 80%, it is crucial to acknowledge that this drop in gel content is not directly correlated to properties such as swelling ratio and bioactive properties, which are crucial to wound healing potential.

The preferred porosity of the scaffolds is generally in the range of 60–90% for tissue engineering applications.<sup>70</sup> The porous scaffold of hydrogel facilitates wound exudate absorption, nutrient distribution, and a stimulating environment for cell proliferation.<sup>18</sup> The porosity of the hydrogels in this study was in the same range of 65–85% which emphasizes its suitability for tissue engineering applications. Interestingly, Ch/PVA<sub>10</sub> hydrogels were less porous than Ch/PVA<sub>5</sub> hydrogels ( $p < 0.05$ ) which can be simply explained as the presence of more PVA in the same volume of hydrogel (Fig. 3c). This result can be associated with crosslinking density or gel content. With the increase in cross-linking density, the distance between the PVA network decreases and forms a more compact structure. In addition, the hydrogel structure is governed by solution viscosity, and increasing the crosslinking degree can result in viscous, dense, and compact hydrogel with smaller pores.<sup>71</sup>

Furthermore, with the increasing amount of collagen peptide in each group of Ch/PVA<sub>5</sub> or Ch/PVA<sub>10</sub> hydrogels, porosity is further decreased. This is attributed to the presence of collagen peptide, which could be filling up the pores and a similar effect can be seen in other Ch/PVA-based hydrogels.<sup>72</sup>

Fig. 3a and c show that for higher collagen peptide and PVA amounts per unit volume, swelling ratios increased, yet porosities show a decrease. One would anticipate that the swelling ratio would increase for the hydrogels with higher porosity but the results are quite the opposite, because swelling is also a function of how tightly the polymer networks are cross-linked. This behavior can be further explained by the movement and realignment of the networks within the hydrogel during swelling independent of the porosity of the hydrogel.<sup>65</sup>

The water evaporation rate is an important assessment to understand the water retention capacity of the hydrogel. Hydrogel dressings should exhibit a lower evaporation rate for faster healing, less pain, and greater cost savings.<sup>73</sup> According to Fig. 3d and e, Ch/PVA<sub>10</sub> hydrogels could retain water better than Ch/PVA<sub>5</sub> hydrogels. It can be observed from Ch/PVA<sub>5</sub> (Fig. 3d) and Ch/PVA<sub>10</sub> (Fig. 3e) that neat Ch/PVA hydrogels without collagen peptide (Ch/PVA<sub>5</sub>-CP<sub>0</sub>, Ch/PVA<sub>10</sub>-CP<sub>0</sub>) demonstrated more water evaporation than collagen peptide-loaded hydrogels; interestingly, a lower amount of collagen peptide showed lower evaporation and better water retention capacity. This corroborates the hypothesis from other characterization studies, that increasing the collagen peptide content causes increasingly denser and more compact hydrogels, with a decrease in water retention. An optimum hydrogel composition of the Ch/PVA to collagen peptide should be chosen with a lower evaporation rate (higher retention) and high swelling ratio and this is shown by Ch/PVA<sub>5</sub>-CP<sub>2</sub>.

**3.2.3 Mechanical and morphological properties.** Hydrogels should have good mechanical properties to cope with the dynamic stretching of skin. Compressive tests were performed to evaluate the mechanical properties of the hydrogel dressings, as this method is more relevant to their clinical application. Hydrogels are soft, non-load-bearing materials that primarily experience compressive forces when applied to wounds. As noted by Boateng *et al.* (2008), compressive testing is commonly used to characterize foam and hydrogel dressings, while tensile testing is typically reserved for film-based or structural formulations.<sup>74</sup> Since PVA provides additional reinforcement to the structure, increasing PVA (Ch/PVA<sub>10</sub>) resulted in the expected improvement of mechanical properties that elevated the fracture stress and compressive modulus of the Ch/PVA<sub>10</sub> hydrogels as compared to Ch/PVA<sub>5</sub> hydrogels formulations, as evident from Fig. 4a–c. In the Ch/PVA<sub>5</sub> hydrogels, increasing the collagen peptide did not improve the fracture stress (Fig. 4a), conversely for Ch/PVA<sub>10</sub> hydrogels, fracture stress improves with the increasing amount of collagen peptide (Fig. 4b). This behavior can be associated with the formation of a greater number of hydrogen bonds and a subsequent reduction in the pore size,<sup>30</sup> which has already been demonstrated for Ch/PVA<sub>10</sub> hydrogels in Fig. 3c. Peng *et al.* (2019) also demonstrated that in hydrogels composed of PVA and chitosan combined with bone marrow mesenchymal stem cells, the compressive strength



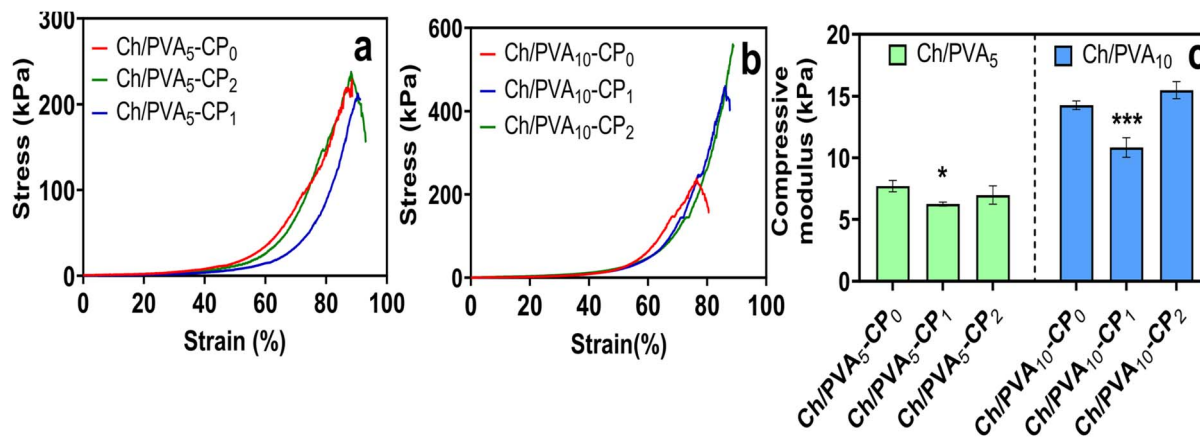


Fig. 4 Mechanical properties of hydrogel; stress–strain curves for (a) Ch/PVA<sub>5</sub> hydrogels, and (b) Ch/PVA<sub>10</sub> hydrogels – unlike Ch/PVA<sub>5</sub> hydrogels, the Ch/PVA<sub>10</sub> hydrogels fracture stress improves with an increasing amount of collagen peptide. (c) Compressive modulus of hydrogels – with a lower amount of collagen peptide loading, the cross-linked network is more elastic, but increasing the amount of collagen peptide contributed to the cross-linking and formed comparatively rigid hydrogels. Error bars represent the means standard error for  $n = 3$  and \* $p < 0.05$ , \*\* $p < 0.01$ , and \*\*\* $p < 0.001$  compared with Ch/PVA<sub>5</sub>-CP<sub>0</sub> and Ch/PVA<sub>10</sub>-CP<sub>0</sub> as controls for corresponding groups.

increased with higher PVA content.<sup>62</sup> Nevertheless, it is recommended to choose the best PVA/chitosan ratio based on various crucial attributes rather than solely focusing on the best mechanical properties.<sup>62</sup> Improved fracture stress of Ch/PVA<sub>10</sub>-CP<sub>1</sub>, and Ch/PVA<sub>10</sub>-CP<sub>2</sub> hydrogels compared to no collagen peptide hydrogel (Ch/PVA<sub>10</sub>-CP<sub>0</sub>) also indicates that collagen peptide-loaded hydrogels are more flexible than the no collagen peptide gels (Fig. 4b). This behavior can be explained by the hydrogen bonding or intermolecular attraction between polymers. During compression, collagen peptide-loaded in the hydrogel realigns to rearrange the chitosan/PVA backbone. Although adding peptides does not improve the mechanical properties as much as polyvinyl alcohol (PVA), as seen in Fig. 4a–c, the collagen peptides help stabilize the network by the hydrogen bonds. This interaction offers some improvement in fracture stress but has little effect on the compressive modulus.

According to Fig. 4c, for an increasing amount of collagen peptide-loaded in both Ch/PVA<sub>5</sub> and Ch/PVA<sub>10</sub> hydrogels, compressive moduli decreased gradually, hit a trough, and then increased again. The findings indicate that with lower levels of collagen peptide loading, the cross-linked network is more elastic, but increasing the amount of collagen peptide contributed to the cross-linking and formed comparatively rigid hydrogels. During compression testing, chitosan polymer absorbed a large amount of fracture energy, and the PVA polymer contributed to maintaining the structure of the hydrogel, which contributed to the perfect mechanical properties of hydrogels.<sup>63</sup> It is important to note that the strong mechanical properties of hydrogels may hamper tissue regeneration on the grafted gel surface due to shearing stress.<sup>62</sup> Hence, Ch/PVA<sub>5</sub>-CP<sub>2</sub> may be considered an optimal choice as it retains both the desired mechanical strength and plasticizing effect.

Following lyophilization, SEM analysis revealed highly interconnected pore networks with robust crosslinking inside the hydrogel suitable as a nano-scaffold (Fig. 5). Although the images suggest a substantial degree of crosslinking, no

regularity in the network can be observed. PVA forms a hexagonal network by bonding with water molecules upon freezing. The freeze-thaw process induces polymer crystallization, partial alignment of molecular chains, and formation of ordered regions called lamellae, which then aggregate into larger structures known as spherulites.<sup>64</sup> Repeated freeze-thaw cycles generate a porous network within the hydrogel, with polymer crystallites serving as junction points that strengthen the structure.<sup>75</sup> This technique forms hydrogen bonds among PVA molecules and yields a porous three-dimensional structure with better mechanical properties.<sup>76</sup> When a chitosan/PVA structure is cross-linked *via* the freeze-thaw cycle, the introduction of chitosan possibly leads to a decrease in the degree of crystallinity of PVA and disrupts the formation of a uniform PVA network.<sup>77</sup> In our scenario, both chitosan and collagen peptide contribute to disrupting the network structure as can be seen from gel content studies. Furthermore, Ch/PVA<sub>10</sub> hydrogels appear to be more defined, and highly crosslinked compared to Ch/PVA<sub>5</sub> hydrogels suggesting the influence of a higher amount of PVA. Noticeably, there were no aggregates or visible buildups inside pores which indicates the homogeneous dispersion and integration of CP with the structure facilitated by effective interaction with PVA and chitosan. The open porous structure of hydrogel is necessary for exudate absorption, nutrient transport, cell adhesion, growth, and proliferation, and overall, accelerating wound healing.<sup>78</sup> Interestingly, when the porosity of hydrogel was tested using ethanol, Ch/PVA<sub>10</sub> hydrogels exhibited lower porosity than Ch/PVA<sub>5</sub> hydrogels (Fig. 3c). Since no regular network is observed in the images, a definitive correlation between porosity and PVA content in the gel would be difficult to ascertain from the SEM images only.

### 3.3 *In vitro* bioactive properties of hydrogels

The *in vitro* anti-inflammatory assay indirectly measures inflammation by considering that tissue protein denaturation, *i.e.*, losing the secondary, tertiary, and quaternary structure of



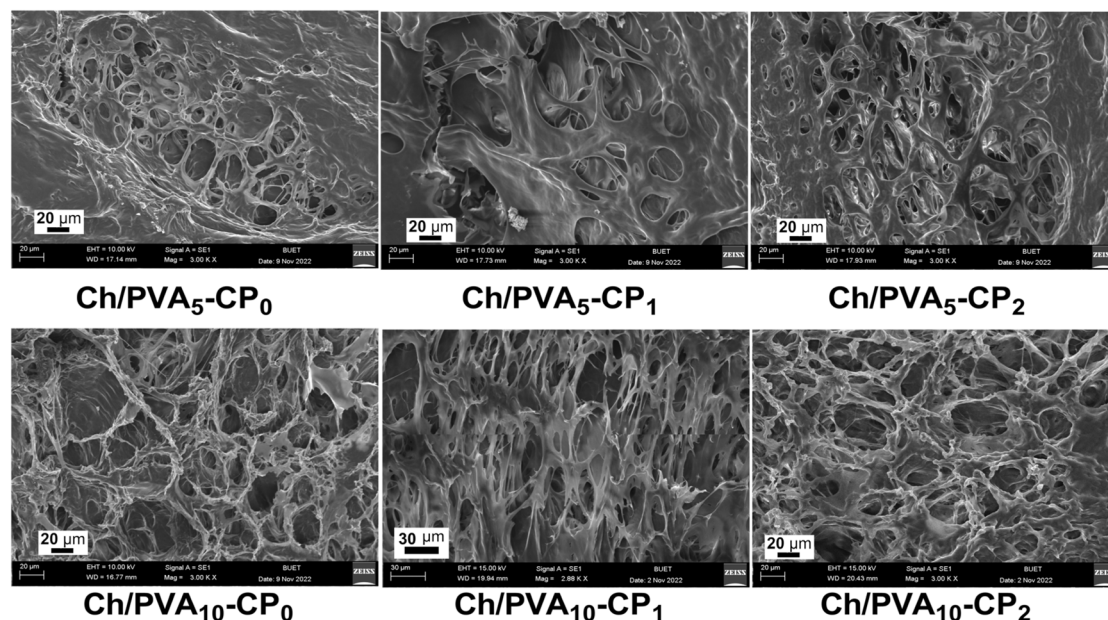


Fig. 5 SEM images of hydrogels for Ch/PVA<sub>5</sub> hydrogels (top row), Ch/PVA<sub>10</sub> (bottom row), and Ch: CP of 1:0, 1:1, and 1:2 combinations (arranged left to right, respectively). The images suggest a substantial degree of irregular crosslinking in the hydrogel. (Ch- Chitosan, CP- Collagen Peptide).

the protein, can culminate into inflammation.<sup>44,79</sup> The hydrogels were tested using bovine serum albumin (BSA) denaturation assay by inducing BSA denaturation at 37 °C incubation. Although it is well known that BSA unfolds above 65°C,<sup>80</sup> at pH 7.0 and temperatures above 30 °C the amount of  $\alpha$ -helix decreases, and  $\beta$ -structure and disordered structure gradually increases.<sup>81</sup> The highest BSA denaturation inhibition was observed for Ch/PVA<sub>5</sub>-CP<sub>2</sub> (44.9 ± 2.4%) and Ch/PVA<sub>10</sub>-CP<sub>2</sub> (43.3 ± 2.83%). BSA denaturation inhibition potential for Ch/PVA<sub>5</sub>-CP<sub>1</sub> (42 ± 2.76%) was close to Ch/PVA<sub>5</sub>-CP<sub>2</sub>. Apart from these, Ch/PVA<sub>10</sub>-CP<sub>1</sub> showed good anti-inflammatory activity (>30%). In a previous study, carboxymethylcellulose hydrogels containing silver nanoparticles were found to inhibit BSA denaturation by 53 ± 0.6%.<sup>44</sup> Among the tested hydrogels, Ch/PVA<sub>5</sub> showed overall better performance than Ch/PVA<sub>10</sub> ( $p < 0.05$ ) (Fig. 6b). For a particular Ch/PVA group, anti-inflammatory activity showed a positive correlation with the amount of collagen peptide in the gel.

Bacterial infection can disrupt the healing process and be life-threatening, if not intervened at early stages. As a wound dressing, hydrogel should demonstrate antimicrobial properties to fight against bacterial infection and protect the wound.<sup>82</sup> The antibacterial test for formulated hydrogels against *E. coli* and *S. aureus* revealed that the zone of inhibition for Ch/PVA<sub>5</sub> formulations was greater than Ch/PVA<sub>10</sub> formulations ( $p < 0.05$ ), as illustrated in Fig. 6b, owing to the higher concentrations of chitosan Ch/PVA<sub>5</sub> hydrogels than Ch/PVA<sub>10</sub> hydrogels. For Gram negative bacteria, the zones of inhibitions the Ch/PVA<sub>5</sub> hydrogels were in the range of 13.17 ± 0.33 mm to 14.57 ± 0.24 mm, significantly higher than for Ch/PVA<sub>10</sub> hydrogels which showed 11.57 ± 0.33 mm to 12.93 ± 0.4 mm. For the Gram-positive bacteria, the zones of inhibitions of the Ch/PVA<sub>5</sub>

hydrogels were in the range of 14.67 ± 0.85 mm to 16 ± 0.41 mm. Compared to this, the Ch/PVA<sub>10</sub> hydrogels showed zone of inhibition in between 12.73 ± 0.21 mm to 13.93 ± 0.33 mm, which were lower than those for the Ch/PVA<sub>5</sub> hydrogels. In a study with chitosan-gelatin based hydrogels the disk-diffusion zones of inhibition against *E. coli* and *S. aureus* were approximately in the range of 10 to 12 mm and 6 to 8 mm, respectively.<sup>83</sup> These results are quite similar to our findings.

Furthermore, the antibacterial properties of the hydrogels did not significantly change with the varying amount of collagen peptide in different formulations. No antibacterial property of the collagen peptide was found against *E. coli* and *S. aureus* in the broth dilution method (see Fig. S2 in SI). Images of the disk diffusion test of hydrogels are attached in the Fig. S3. Therefore, the antibacterial properties of the hydrogels can be solely attributed to chitosan, a biomolecule with broad-spectrum antibacterial properties.<sup>30</sup> While chitosan has excellent antibacterial properties it is also noticeable in Fig. S2 that the inhibition zone was limited because of poor spreadability of chitosan<sup>35</sup> through agar medium. Positively charged chitosan can react with negatively charged surface components on the bacterial cell causing membrane disruption, cell permeation, and eventually, cell death.<sup>84</sup> It is to be noted that a similar study done using hydrogels composed of chitosan, PVA and commercially available peptides showed good cytocompatibility with mammalian cells. When selecting an ideal candidate for a wound dressing, the primary focus should be its bioactive properties. Ch/PVA<sub>5</sub>-CP<sub>2</sub> can be a promising choice for wound dressing considering the exceptional anti-inflammatory, antioxidant (attributed to high collagen peptide content), and antibacterial (stemming from high chitosan content) activity and therefore selected as the treatment in animal trials.



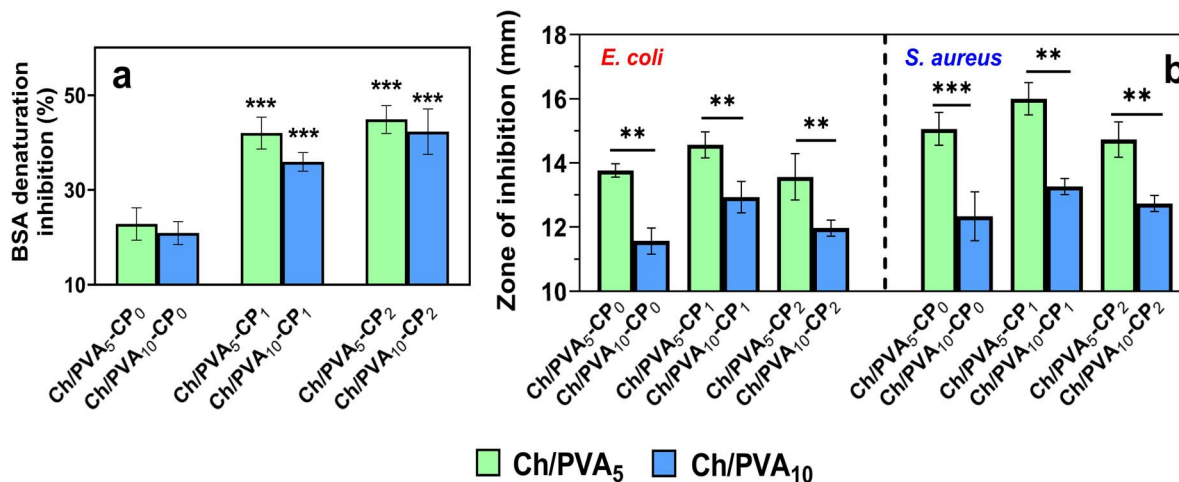


Fig. 6 Bioactive properties of hydrogels. (a) Anti-inflammatory activity to inhibit Bovine Serum Albumin (BSA) denaturation-anti-inflammatory activity demonstrated a positive correlation with the collagen peptide concentration in the gel (b) antibacterial activity against *E. coli*, and *S. aureus* – better antibacterial activity can be observed for Ch/PVA<sub>5</sub> hydrogels owing to the higher amount of chitosan per unit mass of hydrogel. Error bars represent the means standard error for  $n = 3$  and  $*p < 0.05$ ,  $**p < 0.01$ , and  $***p < 0.001$ .

### 3.4 *In vivo* wound healing evaluation

Preliminary *in vivo* studies were carried out using Ch/PVA<sub>5</sub>-CP<sub>2</sub> hydrogel as a burn wound treatment on mice subjects, divided into three groups (test; positive control, *i.e.* Silver sulfadiazine 1%; and negative control, *i.e.* no treatment). Silver sulfadiazine is a sulfonamide-containing antibacterial agent and is usually used to prevent, manage, and treat burn wound infections.<sup>85</sup> In this study, we initially tested two mice from each group (denoted in SI figures as mice of Batch 1 and Batch 2) for 7 days, then investigated one mouse from each group further for 14 days (denoted in SI figures as Batch 3). For comparison for the first 7 days, the results are shown in Fig. 7. On the second day after the wounds were made, wounds on all the animals displayed swelling and an increase in wound area as the natural

inflammatory response of the body increased blood flow to the area.<sup>86</sup> The initial average burn wound area for all groups and batches was approximately  $1.5 \pm 0.15$ .<sup>85</sup> By the end of 7 days, the average wound size of the animals treated with the hydrogel decreased by approximately 20% of its initial size in all batches, with the lowest wound area measuring about  $1.23 \text{ cm}^2$ . Detailed photographs and figures and details of results of these preliminary animal trials can be found in the SI (Fig S4–Fig S7). In the batch of mice tested for 14 days, the initial swelling for the hydrogel was higher however, at the end of the trial period, for the animals treated with Ch/PVA<sub>5</sub>-CP<sub>2</sub>, the wound size reduced to less than 50% of its initial size for the hydrogel-treated group. On the other hand, the negative control animals showed an average final area of around  $1.3 \text{ cm}^2$ , and

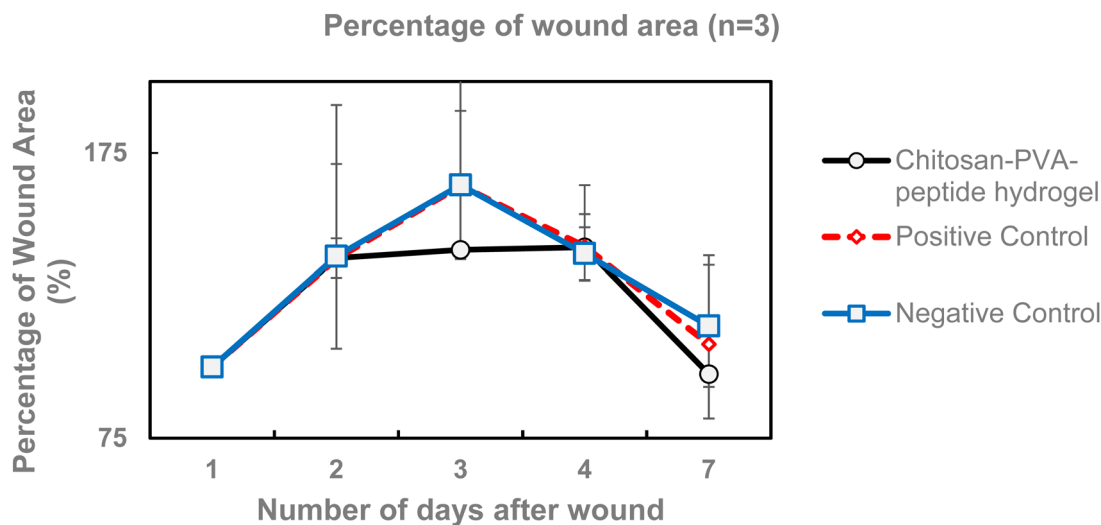


Fig. 7 Healing rate comparison for random mice from two batches observed for 7 days. For all batches, mice were divided into three groups, the black profile shows the results for the group receiving chitosan-PVA-peptide hydrogel, red shows the results for the group receiving commercial ointment, and the blue shows the group receiving no treatment.



the positive controls showed a final area of 1.1 cm<sup>2</sup>. Although the results of this study have not included animal trials with chitosan-PVA with no peptide hydrogel, similar results have been shown in studies using chitosan or chitosan/PVA based hydrogels where the wound area decreases by 20% to 80% during 7 and 14 days.<sup>87,88</sup>

A summary of the results show that the hydrogel can offer enhanced healing compared to untreated healing, and in some cases, even higher healing rates as compared to a commercial ointment. However, more rigorous animal trials must be carried out to determine the healing efficacy and histological studies must be carried out to prove the superior nature of healing of the hydrogels.

## 4 Conclusion

Marine collagen peptide was extracted from locally sourced *Channa striatus* skin, which is typically an aquaculture waste product. The peptides were extracted utilizing enzyme hydrolysis, and the product retained 53.31% protein according to Bradford assay. ATR-FTIR of the extracted peptide confirmed the existence of characteristic amide bonds, representing a random coil structure. SEM images revealed the morphology of the extracted peptide and showed open structure indicating lower molecular weight of the peptide resulting from enzymatic hydrolysis. The salient features of the collagen peptide (CP) includes its enhanced antioxidant activity against DPPH radical, hydroxide radical, and superoxide free radicals. The amino acid profile showed 27.3% glycine, 8.74% arginine, and 14.11% proline, matching the amino acid profile of collagen peptide as found in the literature. Glycine is critical for lipid metabolism, immune regulation, and neurotransmission. It offers good biocompatibility, biodegradability, and strong mechanical properties and can enhance immunity, reduce inflammation, promote wound healing, and improve neurological function. Proline is vital for collagen synthesis and production of biologically active molecules which is also a precursor of arginine.<sup>52</sup> These properties of the collagen peptide indicate that highly bioactive collagen peptide can be yielded from local marine sources through a facile extraction process. Incorporating the collagen peptide into chitosan/PVA hydrogels prepared *via* a non-toxic freeze-thaw process further showcased the sustainable preparation of hydrogel structures for biological applications. The various blends of chitosan/PVA-collagen peptide were investigated to find a structure that showed highly robust mechanical properties yet showed swelling ratios and water retention properties conducive to accelerated wound healing.

Two groups of hydrogels with chitosan/PVA ratio of 1 : 5 and 1 : 10 weight ratio with increasing collagen peptide in each group (chitosan/collagen peptide ratio 1 : 0, 1 : 1, and 1 : 2) were investigated. Ch/PVA<sub>5</sub> hydrogels demonstrated better swelling capacity that increased with increasing amount of incorporated collagen peptide in each group. SEM images of the freeze-dried hydrogels verified the highly porous and irregular network ideal for wound exudate absorption and nutrient transfer. The incorporation of collagen peptide disrupted the network, decreasing the cross-linking (gel content)

as compared to neat chitosan-PVA hydrogels. Incorporation of collagen peptide caused higher swelling and we hypothesize it is due to more hydrogen bonds of the collagen peptide with water molecules owing to the presence of amino acids with large side chains<sup>89</sup> (like arginine, glutamic acid), hydroxy groups<sup>90</sup> (like serine, threonine), and positively charged residues<sup>91</sup> (like lysine, arginine). Regardless of collagen peptide content, increasing the PVA amount in the hydrogel showed higher gel content, resulting in compact hydrogel structures with lower porosity and swelling. FTIR spectra hint at collagen peptide forming bonds with chitosan and PVA *via* electrostatic interaction and hydrogen bond which may have resulted in reduced porosity by dense packing of materials within the three-dimensional network. The swelling ratio is the key structural property of hydrogel for wound healing applications, and Ch/PVA<sub>5</sub>-CP<sub>2</sub> showed a maximum swelling of 619%. For topical applications, mechanically stable hydrogels mimicking the elasticity of the skin are desired and Ch/PVA<sub>5</sub> hydrogels were more elastic in terms of compressive modulus. The compressive modulus of the hydrogels revealed that lower concentrations of collagen peptide had a plasticizing effect on the gels. The Ch/PVA<sub>5</sub>-CP<sub>2</sub> hydrogel is promising for wound healing for its antibacterial properties against *E. coli* (13.6 ± 0.6 mm inhibition zone) and *S. aureus* (14.7 ± 0.4 mm inhibition zone), antioxidant (hydroxyl, superoxide, and DPPH scavenging) effects, anti-inflammatory (44.9 ± 2.9%) effects, and a good balance of strength and elasticity. Based on preliminary animal trials conducted on mice, Ch/PVA<sub>5</sub>-CP<sub>2</sub> demonstrated superior performance compared to both commercial burn ointment (silver sulfadiazine 1%, positive control) and no treatment (negative control), thereby, highlighting the potential of chitosan-PVA hydrogels incorporating locally sourced bioactive collagen peptide as a burn wound treatment. However, there is scope for further improvement of collagen peptide extraction yields, exploring additional combinations of extracted collagen peptide in the hydrogel, purifying and sequencing the most potent bioactive collagen peptide from the blend of extracted collagen peptides, and conducting comprehensive animal trials. Further research is worthwhile since the hydrogels of the study are formulated from waste skin of local fish and thus can play a positive role in circular economy such fishing sector wastes.

## Ethical statement

All animal experiments complied with ARRIVE (Animal Research: Reporting of *In Vivo* Experiments) guidelines. The study was conducted in accordance with the U.K. Animals (Scientific Procedures) Act, 1986, its associated guidelines, and the EU Directive 2010/63 for the protection of animals used for scientific purposes. The experimental procedures were approved by the Animal Ethics Committee of the Department of Chemical Engineering, Bangladesh University of Engineering and Technology (BUET/CHE/A2402). Female Swiss albino mice were used in this study following the NIH (National Research Council) Guide for the Care and Use of Laboratory Animals.



## Author contributions

Tanjina Tarannum: data curation (lead), formal analysis (lead), investigation (lead), methodology (equal), validation (lead), writing – original draft (lead); Farhana Islam: formal analysis (support), investigation (lead), methodology (equal), writing – original draft (support). Khondoker Kabbyo Shariar: data curation (support). Formal analysis (support), validation (support), writing – original draft (support). Nafisa Islam: conceptualization, funding acquisition, project administration, resources, supervision, validation (support), visualization, writing – review and editing.

## Conflicts of interest

There are no conflicts to declare.

## Data availability

The data can be obtained from the corresponding author upon reasonable request. Supplementary information is available. See DOI: <https://doi.org/10.1039/d5ra05717e>. The Supplementary information document contains FTIR spectra of the collagen peptide extracted from the Snakehead fish and compares it to the spectra of commercially available marine collagen peptide. The document also has detailed images of the antibacterial tests and of the preliminary animal trials involving the hydrogel peptides, along with healing rate comparisons for 7 and 14 days.

## Acknowledgements

This research was supported by a grant from UNESCO (4500429395) and the International Development Research Centre (IDRC) in Ottawa, Canada. The research assistantship funding was partially provided by Committee for Advanced Studies and Research, (CASR), BUET. The authors wish to express their gratitude to the Applied Bioengineering Research Incubator (ABRI) BUET and Bangladesh University (BU) for providing access to their facilities.

## References

- 1 S. Natarajan, D. Williamson, A. J. Stiltz and K. G. Harding, Advances in wound care and healing technology, *Am. J. Clin. Dermatol.*, 2000, **1**(5), 269–275, DOI: [10.2165/00128071-200001050-00002](https://doi.org/10.2165/00128071-200001050-00002).
- 2 J. E. Alonso, J. Lee, A. R. Burgess and B. D. Browner, The management of complex orthopedic injuries, *Surg. Clin. North Am.*, 1996, **76**(4), 879–903, DOI: [10.1016/S0039-6109\(05\)70486-2](https://doi.org/10.1016/S0039-6109(05)70486-2).
- 3 S. Dhivya, V. V. Padma and E. Santhini, Wound dressings - A review, *Biomedicine*, 2015, **5**(4), 22, DOI: [10.7603/s40681-015-0022-9](https://doi.org/10.7603/s40681-015-0022-9).
- 4 N. Shanmugasundaram, T. S. Uma, T. S. R. Lakshmi and M. Babu, Efficiency of controlled topical delivery of silver sulfadiazine in infected burn wounds, *J. Biomed. Mater. Res., Part A*, 2009, **89A**(2), 472–482, DOI: [10.1002/jbm.a.31997](https://doi.org/10.1002/jbm.a.31997).
- 5 R. M. Johnson and R. Richard, Partial-thickness burns: identification and management, *Adv. Skin Wound Care*, 2003, **16**(4), 178–187, DOI: [10.1097/00129334-200307000-00011](https://doi.org/10.1097/00129334-200307000-00011).
- 6 C. K. Field and M. D. Kerstein, Overview of wound healing in a moist environment, *Am. J. Surg.*, 1994, **167**(1), 52–56, DOI: [10.1016/0002-9610\(94\)90002-7](https://doi.org/10.1016/0002-9610(94)90002-7).
- 7 E. Öhnstedt, H. Lofton Tomenius, E. Vågesjö and M. Phillipson, The discovery and development of topical medicines for wound healing, *Expert Opin. Drug Discovery*, 2019, **14**(5), 485–497, DOI: [10.1080/17460441.2019.1588879](https://doi.org/10.1080/17460441.2019.1588879).
- 8 N. A. Peppas and A. R. Khare, Preparation, structure and diffusional behavior of hydrogels in controlled release, *Adv. Drug Delivery Rev.*, 1993, **11**, 1–35, DOI: [10.1016/0169-409X\(93\)90025-Y](https://doi.org/10.1016/0169-409X(93)90025-Y).
- 9 S. Mukherji, J. Ruparelia, and S. Agnihotri, Antimicrobial activity of silver and copper nanoparticles: Variation in sensitivity across various strains of bacteria and fungi, in *Nano-Antimicrobials: Progress and Prospects*, 2012, DOI: [10.1007/978-3-642-24428-5\\_8](https://doi.org/10.1007/978-3-642-24428-5_8).
- 10 X. Zhao, H. Wu, B. Guo, R. Dong, Y. Qiu and P. X. Ma, Antibacterial anti-oxidant electroactive injectable hydrogel as self-healing wound dressing with hemostasis and adhesiveness for cutaneous wound healing, *Biomaterials*, 2017, **122**, 34–47, DOI: [10.1016/j.biomaterials.2017.01.011](https://doi.org/10.1016/j.biomaterials.2017.01.011).
- 11 P. Simard, H. Galarneau, S. Marois, *et al.*, Neutrophils exhibit distinct phenotypes toward chitosans with different degrees of deacetylation: implications for cartilage repair, *Arthritis Res. Ther.*, 2009, **11**(3), R74, DOI: [10.1186/AR2703](https://doi.org/10.1186/AR2703).
- 12 C. J. Park, S. G. Clark, C. A. Lichtensteiger, R. D. Jamison and A. J. W. Johnson, Accelerated wound closure of pressure ulcers in aged mice by chitosan scaffolds with and without bFGF, *Acta Biomater.*, 2009, **5**(6), 1926–1936, DOI: [10.1016/j.actbio.2009.03.002](https://doi.org/10.1016/j.actbio.2009.03.002).
- 13 G. I. Howling, P. W. Dettmar, P. A. Goddard, F. C. Hampson, M. Dornish and E. J. Wood, The effect of chitin and chitosan on the proliferation of human skin fibroblasts and keratinocytes in vitro, *Biomaterials*, 2001, **22**(22), 2959–2966, DOI: [10.1016/S0142-9612\(01\)00042-4](https://doi.org/10.1016/S0142-9612(01)00042-4).
- 14 J. Fu, F. Yang and Z. Guo, The chitosan hydrogels: from structure to function, *New J. Chem.*, 2018, **42**(21), 17162–17180, DOI: [10.1039/C8NJ03482F](https://doi.org/10.1039/C8NJ03482F).
- 15 G. Li, Q. Yan, H. Xia and Y. Zhao, Therapeutic-Ultrasound-Triggered Shape Memory of a Melamine-Enhanced Poly(vinyl alcohol) Physical Hydrogel, *ACS Appl. Mater. Interfaces*, 2015, **7**(22), 12067–12073, DOI: [10.1021/ACSAMI.5B02234/SUPPL\\_FILE/AM5B02234\\_SI\\_001](https://doi.org/10.1021/ACSAMI.5B02234/SUPPL_FILE/AM5B02234_SI_001).
- 16 K. Enoch, R. C. S and A. A. Somasundaram, Improved mechanical properties of Chitosan/PVA hydrogel – A detailed Rheological study, *Surf. Interfaces*, 2023, **41**, 103178, DOI: [10.1016/j.surfin.2023.103178](https://doi.org/10.1016/j.surfin.2023.103178).
- 17 S. Wu, L. Deng, H. Hsia, *et al.*, Evaluation of gelatin-hyaluronic acid composite hydrogels for accelerating



- wound healing, *J. Biomater. Appl.*, 2017, **31**(10), 1380–1390, DOI: [10.1177/0885328217702526](https://doi.org/10.1177/0885328217702526).
- 18 K. Kalantari, E. Mostafavi, B. Saleh, P. Soltantabar and T. J. Webster, Chitosan/PVA hydrogels incorporated with green synthesized cerium oxide nanoparticles for wound healing applications, *Eur. Polym. J.*, 2020, **134**, 109853, DOI: [10.1016/j.eurpolymj.2020.109853](https://doi.org/10.1016/j.eurpolymj.2020.109853).
- 19 J. L. Soriano, A. C. Calpena, M. J. Rodríguez-Lagunas, *et al.*, Endogenous antioxidant cocktail loaded hydrogel for topical wound healing of burns, *Pharmaceutics*, 2021, **13**(1), 8, DOI: [10.3390/pharmaceutics13010008](https://doi.org/10.3390/pharmaceutics13010008).
- 20 S. H. Jeong, S. Cheong, T. Y. Kim, H. Choi and S. K. Hahn, Supramolecular Hydrogels for Precisely Controlled Antimicrobial Peptide Delivery for Diabetic Wound Healing, *ACS Appl. Mater. Interfaces*, 2023, **15**(13), 16471–16481, DOI: [10.1021/acsami.3c00191](https://doi.org/10.1021/acsami.3c00191).
- 21 S. Li, Q. Dong, X. Peng, *et al.*, Self-Healing Hyaluronic Acid Nanocomposite Hydrogels with Platelet-Rich Plasma Impregnated for Skin Regeneration, *ACS Nano*, 2022, **16**(7), 11346–11359, DOI: [10.1021/acsnano.2c05069](https://doi.org/10.1021/acsnano.2c05069).
- 22 S. Addad, J. Y. Exposito, C. Faye, S. Ricard-Blum and C. Lethias, Isolation, characterization and biological evaluation of jellyfish collagen for use in biomedical applications, *Mar. Drugs*, 2011, **9**(6), 967–983, DOI: [10.3390/md9060967](https://doi.org/10.3390/md9060967).
- 23 A. Clemente, Enzymatic protein hydrolysates in human nutrition, *Trends Food Sci. Technol.*, 2000, **11**(7), 254–262, DOI: [10.1016/S0924-2244\(01\)00007-3](https://doi.org/10.1016/S0924-2244(01)00007-3).
- 24 L. Fan, M. Cao, S. Gao, *et al.*, Preparation and characterization of sodium alginate modified with collagen peptides, *Carbohydr. Polym.*, 2013, **93**(2), 380–385, DOI: [10.1016/j.carbpol.2013.01.029](https://doi.org/10.1016/j.carbpol.2013.01.029).
- 25 K. Dybka-Stępień, P. Walczak and M. Turkiewicz, Collagen hydrolysates as a new diet supplement, *Food Chem. Biotechnol.*, 2009, **73**(11530002), 83–92.
- 26 Z. Hu, P. Yang, C. Zhou, S. Li and P. Hong, Marine collagen peptides from the skin of Nile Tilapia (*Oreochromis niloticus*): Characterization and wound healing evaluation, *Mar. Drugs*, 2017, **15**(4), 102, DOI: [10.3390/md15040102](https://doi.org/10.3390/md15040102).
- 27 M. Pozzolini, E. Millo, C. Oliveri, *et al.*, Elicited ROS scavenging activity, photoprotective, and wound-healing properties of collagen-derived peptides from the marine sponge *Chondrosia reniformis*, *Mar. Drugs*, 2018, **16**(12), 465, DOI: [10.3390/md16120465](https://doi.org/10.3390/md16120465).
- 28 A. Kumar, T. Behl and S. Chadha, Synthesis of physically crosslinked PVA/Chitosan loaded silver nanoparticles hydrogels with tunable mechanical properties and antibacterial effects, *Int. J. Biol. Macromol.*, 2020, **149**, 1262–1274, DOI: [10.1016/j.ijbiomac.2020.02.048](https://doi.org/10.1016/j.ijbiomac.2020.02.048).
- 29 Q. Q. Ouyang, Z. Hu, Z. P. Lin, *et al.*, Chitosan hydrogel in combination with marine peptides from tilapia for burns healing, *Int. J. Biol. Macromol.*, 2018, **112**, 1191–1198, DOI: [10.1016/j.ijbiomac.2018.01.217](https://doi.org/10.1016/j.ijbiomac.2018.01.217).
- 30 X. H. Zhang, Z. Yin, Y. Guo, *et al.*, A facile and large-scale synthesis of a PVA/chitosan/collagen hydrogel for wound healing, *New J. Chem.*, 2020, **44**(47), 20776–20784, DOI: [10.1039/d0nj04016a](https://doi.org/10.1039/d0nj04016a).
- 31 B. Ge, H. Wang, J. Li, *et al.*, Comprehensive Assessment of Nile Tilapia Skin (*Oreochromis niloticus*) Collagen Hydrogels for Wound Dressings, *Mar. Drugs*, 2020, **18**(4), 178, DOI: [10.3390/md18040178](https://doi.org/10.3390/md18040178).
- 32 M. do L. L. R. Menezes, H. L. Ribeiro, F. de O. M. da S. Abreu, J. P. de A. Feitosa and M. de S. M. de S. Filho, Optimization of the collagen extraction from Nile tilapia skin (*Oreochromis niloticus*) and its hydrogel with hyaluronic acid, *Colloids Surf., B*, 2020, **189**, 110852, DOI: [10.1016/j.colsurfb.2020.110852](https://doi.org/10.1016/j.colsurfb.2020.110852).
- 33 Y. Luo, M. Fu, Z. Zhou, *et al.*, A tilapia skin-derived gelatin hydrogel combined with the adipose-derived stromal vascular fraction for full-thickness wound healing, *Nanoscale Adv.*, 2024, **6**(16), 4230–4236, DOI: [10.1039/D4NA00332B](https://doi.org/10.1039/D4NA00332B).
- 34 O. Qianqian, K. Songzhi, H. Yongmei, *et al.*, Preparation of nano-hydroxyapatite/chitosan/tilapia skin peptides hydrogels and its burn wound treatment, *Int. J. Biol. Macromol.*, 2021, **181**, 369–377, DOI: [10.1016/j.ijbiomac.2021.03.085](https://doi.org/10.1016/j.ijbiomac.2021.03.085).
- 35 T. C. Sun, B. Y. Yan, X. C. Ning, *et al.*, A nanofiber hydrogel derived entirely from ocean biomass for wound healing, *Nanoscale Adv.*, 2022, **5**(1), 160–170, DOI: [10.1039/D2NA00535B](https://doi.org/10.1039/D2NA00535B).
- 36 M. A. K. Haniffa, P. A. Jeya Sheela, K. Kavitha and A. M. M. Jais, Salutary value of haruan, the striped snakehead *Channa striatus* - A review, *Asian Pac. J. Trop. Biomed.*, 2014, **4**(May 2014), S8–S15, DOI: [10.12980/APJTB.4.2014C1015](https://doi.org/10.12980/APJTB.4.2014C1015).
- 37 G. K. S. Arumugam, D. Sharma, R. M. Balakrishnan and J. B. P. Ettiyappan, Extraction, optimization and characterization of collagen from sole fish skin, *Sustainable Chem. Pharm.*, 2018, 19–26, DOI: [10.1016/j.scp.2018.04.003](https://doi.org/10.1016/j.scp.2018.04.003).
- 38 N. Ennaas, R. Hammami, L. Beaulieu and I. Fliss, Production of antibacterial fraction from Atlantic mackerel (*Scomber scombrus*) and its processing by-products using commercial enzymes, *Food Bioprod. Process.*, 2015, **96**, 145–153, DOI: [10.1016/j.fbp.2015.07.014](https://doi.org/10.1016/j.fbp.2015.07.014).
- 39 M. M. Bradford, A rapid and sensitive method for the quantitation of microgram quantities of protein utilizing the principle of protein-dye binding, *Anal. Biochem.*, 1976, **72**(1–2), 248–254, DOI: [10.1016/0003-2697\(76\)90527-3](https://doi.org/10.1016/0003-2697(76)90527-3).
- 40 Y. Zhang, X. Duan and Y. Zhuang, Purification and characterization of novel antioxidant peptides from enzymatic hydrolysates of tilapia (*Oreochromis niloticus*) skin gelatin, *Peptides*, 2012, **38**(1), 13–21, DOI: [10.1016/j.peptides.2012.08.014](https://doi.org/10.1016/j.peptides.2012.08.014).
- 41 M. D. Figueroa-Pizano, I. Vélaz and M. E. Martínez-Barbosa, A freeze-thawing method to prepare chitosan-poly(Vinyl alcohol) hydrogels without crosslinking agents and diflunisal release studies, *J. Visualized Exp.*, 2019, **2020**(155), 1–9, DOI: [10.3791/59636](https://doi.org/10.3791/59636).
- 42 F. Islam, E. Rahman, T. Tarannum and N. Islam, Assessment of chitosan-PVA hydrogels infused with marine collagen peptides for potential wound healing applications,



- Compos., Part C: Open Access*, 2024, **15**, 100528, DOI: [10.1016/j.jcomc.2024.100528](https://doi.org/10.1016/j.jcomc.2024.100528).
- 43 L. Liu, H. Wen, Z. Rao, *et al.*, Preparation and characterization of chitosan – collagen peptide/oxidized konjac glucomannan hydrogel, *Int. J. Biol. Macromol.*, 2018, **108**, 376–382, DOI: [10.1016/j.ijbiomac.2017.11.128](https://doi.org/10.1016/j.ijbiomac.2017.11.128).
- 44 M. Ruffo, O. I. Parisi, M. Dattilo, *et al.*, Synthesis and evaluation of wound healing properties of hydro-diab hydrogel loaded with green-synthesized AGNPS: *in vitro* and *in ex vivo* studies, *Drug Delivery Transl. Res.*, 2022, **12**(8), 1881–1894, DOI: [10.1007/s13346-022-01121-w](https://doi.org/10.1007/s13346-022-01121-w).
- 45 Animals NRC (US) C for the U of the G for the C and U of L, Guide for the Care and Use of Laboratory Animals, *Guide for the Care and Use of Laboratory Animals*, Published online December 27, 2011, DOI: [10.17226/12910](https://doi.org/10.17226/12910).
- 46 S. Yano, K. Yamaguchi, M. Shibata, S. Ifuku and N. Teramoto, Photocrosslinked Fish Collagen Peptide/Chitin Nanofiber Composite Hydrogels from Marine Resources: Preparation, Mechanical Properties, and an *In Vitro* Study, *Polymers*, 2023, **15**(3), 682, DOI: [10.3390/POLYM15030682/S1](https://doi.org/10.3390/POLYM15030682/S1).
- 47 A. León-López, L. Fuentes-Jiménez, A. D. Hernández-Fuentes, R. G. Campos-Montiel and G. Aguirre-álvarez, Hydrolysed Collagen from Sheepskins as a Source of Functional Peptides with Antioxidant Activity, *Int. J. Mol. Sci.*, 2019, **20**(16), 3931, DOI: [10.3390/ijms20163931](https://doi.org/10.3390/ijms20163931).
- 48 C. F. Chi, Z. H. Cao, B. Wang, F. Y. Hu, Z. R. Li and B. Zhang, Antioxidant and functional properties of collagen hydrolysates from Spanish mackerel skin as influenced by average molecular weight, *Molecules*, 2014, **19**(8), 11211–11230, DOI: [10.3390/molecules190811211](https://doi.org/10.3390/molecules190811211).
- 49 N. J. Kruger, The Bradford method for protein quantitation, *Methods Mol. Biol.*, 1994, **32**, 9–15, DOI: [10.1385/0-89603-268-x](https://doi.org/10.1385/0-89603-268-x).
- 50 J. J. Sedmak and S. E. Grossberg, A rapid, sensitive, and versatile assay for protein using Coomassie brilliant blue G250, *Anal. Biochem.*, 1977, **79**(1–2), 544–552, DOI: [10.1016/0003-2697\(77\)90428-6](https://doi.org/10.1016/0003-2697(77)90428-6).
- 51 R. W. Congdon, G. W. Muth and A. G. Splittgerber, The binding interaction of coomassie blue with proteins, *Anal. Biochem.*, 1993, **213**(2), 407–413, DOI: [10.1006/abio.1993.1439](https://doi.org/10.1006/abio.1993.1439).
- 52 Y. Ji, W. Song, L. Xu, D. G. Yu and S. W. A. Bligh, A Review on Electrospun Poly(amino acid) Nanofibers and Their Applications of Hemostasis and Wound Healing, *Biomolecules*, 2022, **12**(6), 794, DOI: [10.3390/BIOM12060794](https://doi.org/10.3390/BIOM12060794).
- 53 J. Liu, D. Zhang, Y. Zhu, Y. Wang, S. He and T. Zhang, Enhancing the *in vitro* Antioxidant Capacities via the interaction of amino acids, *Emir. J. Food Agric.*, 2018, **30**(3), 224–231, DOI: [10.9755/efja.2018.v30.i3.1641](https://doi.org/10.9755/efja.2018.v30.i3.1641).
- 54 K. Saito, D. H. Jin, T. Ogawa, *et al.*, Antioxidative properties of tripeptide libraries prepared by the combinatorial chemistry, *J. Agric. Food Chem.*, 2003, **51**(12), 3668–3674, DOI: [10.1021/jf021191n](https://doi.org/10.1021/jf021191n).
- 55 R. G. Frykberg and J. Banks, Challenges in the Treatment of Chronic Wounds, *Adv. Wound Care*, 2015, **4**(9), 560–582, DOI: [10.1089/wound.2015.0635](https://doi.org/10.1089/wound.2015.0635).
- 56 N. A. S. M. Rasimi, N. H. Ishak, I. S. Mannur and N. M. Sarbon, Optimization of enzymatic hydrolysis condition of snakehead (*Channa striata*) protein hydrolysate based on yield and antioxidant activity, *Food Res.*, 2020, **4**(6), 237, DOI: [10.26656/fr.2017.4](https://doi.org/10.26656/fr.2017.4).
- 57 M. M. Schmidt, A. M. da FONTOURA, A. R. Vidal, *et al.*, Characterization of hydrolysates of collagen from mechanically separated chicken meat residue, *Food Sci. Technol.*, 2020, DOI: [10.1590/fst.14819](https://doi.org/10.1590/fst.14819).
- 58 R. Varma and S. Vasudevan, Extraction, characterization, and antimicrobial activity of chitosan from horse mussel modiolus modiolus, *ACS Omega*, 2020, **5**(32), 20224–20230, DOI: [10.1021/ACSOMEGA.0C01903](https://doi.org/10.1021/ACSOMEGA.0C01903).
- 59 H.-Z. Li, S.-C. Chen and Y.-Z. Wang, Preparation and characterization of nanocomposites of polyvinyl alcohol/cellulose nanowhiskers/chitosan, *Compos. Sci. Technol.*, 2015, **115**, 60–65, DOI: [10.1016/j.compscitech.2015.05.004](https://doi.org/10.1016/j.compscitech.2015.05.004).
- 60 M. Hamidi, A. Azadi and P. Rafiei, Hydrogel nanoparticles in drug delivery, *Adv. Drug Delivery Rev.*, 2008, **60**(15), 1638–1649, DOI: [10.1016/j.addr.2008.08.002](https://doi.org/10.1016/j.addr.2008.08.002).
- 61 X. Tong, J. Zheng, Y. Lu, Z. Zhang and H. Cheng, Swelling and mechanical behaviors of carbon nanotube/poly(vinyl alcohol) hybrid hydrogels, *Mater. Lett.*, 2007, **61**(8–9), 1704–1706, DOI: [10.1016/j.matlet.2006.07.115](https://doi.org/10.1016/j.matlet.2006.07.115).
- 62 L. Peng, Y. Zhou, W. Lu, *et al.*, Characterization of a novel polyvinyl alcohol/chitosan porous hydrogel combined with bone marrow mesenchymal stem cells and its application in articular cartilage repair, *BMC Musculoskeletal Disord.*, 2019, **20**(1), 1–12, DOI: [10.1186/S12891-019-2644-7](https://doi.org/10.1186/S12891-019-2644-7).
- 63 S. Bi, P. Wang, S. Hu, *et al.*, Construction of physical-crosslink chitosan/PVA double-network hydrogel with surface mineralization for bone repair, *Carbohydr. Polym.*, 2019, **224**(March), 115176, DOI: [10.1016/j.carbpol.2019.115176](https://doi.org/10.1016/j.carbpol.2019.115176).
- 64 A. Keller, Morphology of Crystallizing Polymers, *Nature*, 1952, **169**(4309), 913–914, DOI: [10.1038/169913a0](https://doi.org/10.1038/169913a0).
- 65 A. Kumar, T. Behl and S. Chadha, Synthesis of physically crosslinked PVA/Chitosan loaded silver nanoparticles hydrogels with tunable mechanical properties and antibacterial effects, *Int. J. Biol. Macromol.*, 2020, **149**, 1262–1274, DOI: [10.1016/j.ijbiomac.2020.02.048](https://doi.org/10.1016/j.ijbiomac.2020.02.048).
- 66 W. Yang, E. Fortunati, F. Bertoglio, *et al.*, Polyvinyl alcohol/chitosan hydrogels with enhanced antioxidant and antibacterial properties induced by lignin nanoparticles, *Carbohydr. Polym.*, 2018, **181**, 275–284, DOI: [10.1016/j.carbpol.2017.10.084](https://doi.org/10.1016/j.carbpol.2017.10.084).
- 67 T. Wikanta, M. Erizal, M. Tjahyono and M. Sugiyono, Synthesis of Polyvinyl Alcohol-Chitosan Hydrogel and Study of Its Swelling and Antibacterial Properties, *Squalen Bull. Mar. Fish. Postharvest Biotechnol.*, 2013, **7**(1), 1, DOI: [10.15578/squalen.v7i1.10](https://doi.org/10.15578/squalen.v7i1.10).
- 68 S. O. Sarrigiannidis, J. M. Rey, O. Dobre, C. González-García, M. J. Dalby and M. Salmeron-Sanchez, A tough act to follow: collagen hydrogel modifications to improve mechanical and growth factor loading capabilities, *Mater. Today Bio*, 2021, **10**, 100098, DOI: [10.1016/j.mtbio.2021.100098](https://doi.org/10.1016/j.mtbio.2021.100098).



- 69 X. Zhang, X. Jiang, B. Tan, X. Zhang, D. Ye and H. Dai, Studies on the properties of poly(vinyl alcohol) film plasticized by urea/ethanolamine mixture, *J. Appl. Polym. Sci.*, 2012, **125**(1), 697–703, DOI: [10.1002/app.34957](https://doi.org/10.1002/app.34957).
- 70 M. Pezeshki-Modaress, M. Zandi and S. Rajabi, Tailoring the gelatin/chitosan electrospun scaffold for application in skin tissue engineering: an *in vitro* study, *Prog. Biomater.*, 2018, **7**(3), 207–218, DOI: [10.1007/s40204-018-0094-1](https://doi.org/10.1007/s40204-018-0094-1).
- 71 S. Spoljaric, A. Salminen, N. D. Luong and J. Seppälä, Stable, self-healing hydrogels from nanofibrillated cellulose, poly(vinyl alcohol) and borax *via* reversible crosslinking, *Eur. Polym. J.*, 2014, **56**(1), 105–117, DOI: [10.1016/j.eurpolymj.2014.03.009](https://doi.org/10.1016/j.eurpolymj.2014.03.009).
- 72 S. P. Lin, K. Y. Lo, T. N. Tseng, J. M. Liu, T. Y. Shih and K. C. Cheng, Evaluation of PVA/dextran/chitosan hydrogel for wound dressing, *Cell. Polym.*, 2019, **38**(1–2), 15–30, DOI: [10.1177/0262489319839211](https://doi.org/10.1177/0262489319839211).
- 73 L. Fan, H. Yang, J. Yang, M. Peng and J. Hu, Preparation and characterization of chitosan/gelatin/PVA hydrogel for wound dressings, *Carbohydr. Polym.*, 2016, 52–57, DOI: [10.1016/j.carbpol.2016.03.002](https://doi.org/10.1016/j.carbpol.2016.03.002).
- 74 J. S. Boateng, K. H. Matthews, H. N. E. Stevens and G. M. Eccleston, Wound healing dressings and drug delivery systems: A review, *J. Pharm. Sci.*, 2008, **97**(8), 2892–2923, DOI: [10.1002/jps.21210](https://doi.org/10.1002/jps.21210).
- 75 R. Ricciardi, F. Auriemma, C. De Rosa and F. Lauprêtre, X-ray Diffraction Analysis of Poly(vinyl alcohol) Hydrogels, Obtained by Freezing and Thawing Techniques, *Macromolecules*, 2004, **37**(5), 1921–1927, DOI: [10.1021/ma035663q](https://doi.org/10.1021/ma035663q).
- 76 H. Park and D. Kim, Swelling and mechanical properties of glycol chitosan/poly (vinyl alcohol) IPN-type superporous hydrogels, *J. Biomed. Mater. Res., Part A*, 2006, **78**(4), 662–667, DOI: [10.1002/jbm.a.30768](https://doi.org/10.1002/jbm.a.30768).
- 77 T. Koyano, N. Koshizaki, H. Umehara, M. Nagura and N. Minoura, Surface states of PVA/chitosan blended hydrogels, *Polymer*, 2000, **41**(12), 4461–4465, DOI: [10.1016/S0032-3861\(99\)00675-8](https://doi.org/10.1016/S0032-3861(99)00675-8).
- 78 Z. Fan, B. Liu, J. Wang, *et al.*, A novel wound dressing based on Ag/graphene polymer hydrogel: Effectively kill bacteria and accelerate wound healing, *Adv. Funct. Mater.*, 2014, **24**(25), 3933–3943, DOI: [10.1002/adfm.201304202](https://doi.org/10.1002/adfm.201304202).
- 79 E. L. OPIE, On the relation of necrosis and inflammation to denaturation of proteins, *J. Exp. Med.*, 1962, **115**(3), 597–608, DOI: [10.1084/JEM.115.3.597](https://doi.org/10.1084/JEM.115.3.597).
- 80 O. S. Nnyigide and K. Hyun, The protection of bovine serum albumin against thermal denaturation and gelation by sodium dodecyl sulfate studied by rheology and molecular dynamics simulation, *Food Hydrocolloids*, 2020, **103**(November 2019), 105656, DOI: [10.1016/j.foodhyd.2020.105656](https://doi.org/10.1016/j.foodhyd.2020.105656).
- 81 K. Takeda, A. Wada, K. Yamamoto, Y. Moriyama and K. Aoki, Conformational change of bovine serum albumin by heat treatment, *J. Protein Chem.*, 1989, **8**, 653–659, DOI: [10.1007/BF01025605](https://doi.org/10.1007/BF01025605).
- 82 H. Cui, M. Liu, W. Yu, *et al.*, Copper Peroxide-Loaded Gelatin Sponges for Wound Dressings with Antimicrobial and Accelerating Healing Properties, *ACS Appl. Mater. Interfaces*, 2021, **13**(23), 26800–26807, DOI: [10.1021/acsami.1c07409](https://doi.org/10.1021/acsami.1c07409).
- 83 B. Farasati Far, M. Reza Naimi-Jamal, M. Jahanbakhshi, A. Hadizadeh and S. Dehghan, Enhanced antibacterial activity of porous chitosan-based hydrogels crosslinked with gelatin and metal ions, *Sci. Rep.*, 2024, **14**, 7505, DOI: [10.1038/s41598-024-58174-9](https://doi.org/10.1038/s41598-024-58174-9).
- 84 S. Agnihotri, S. Mukherji and S. Mukherji, Antimicrobial chitosan–PVA hydrogel as a nanoreactor and immobilizing matrix for silver nanoparticles, *Appl. Nanosci.*, 2012, **2**(3), 179–188, DOI: [10.1007/s13204-012-0080-1](https://doi.org/10.1007/s13204-012-0080-1).
- 85 A. Bult and C. M. Plug, Silver Sulfadiazine, *Anal. Profiles Drug Subst. Excipients*, 2023, **13**(C), 553–571, DOI: [10.1016/S0099-5428\(08\)60202-6](https://doi.org/10.1016/S0099-5428(08)60202-6).
- 86 V. K. Tiwari, Burn wound: How it differs from other wounds, *Indian J. Plast. Surg.*, 2012, **45**(2), 364–373, DOI: [10.4103/0970-0358.101319](https://doi.org/10.4103/0970-0358.101319).
- 87 R. N. M. K. J. P. *et al.*, Enhanced wound healing by PVA/Chitosan/Curcumin patches: *In vitro* and *in vivo* study, *Colloids Surf., B*, 2019, **182**, 110339, DOI: [10.1016/J.COLSURFB.2019.06.068](https://doi.org/10.1016/J.COLSURFB.2019.06.068).
- 88 A. Shamloo, Z. Aghababaie, H. Afjoul, *et al.*, Fabrication and evaluation of chitosan/gelatin/PVA hydrogel incorporating honey for wound healing applications: An *in vitro*, *in vivo* study, *Int. J. Pharm.*, 2021, **592**, 120068, DOI: [10.1016/J.IJPHARM.2020.120068](https://doi.org/10.1016/J.IJPHARM.2020.120068).
- 89 K. Manikandan and S. Ramakumar, The occurrence of C–H...O hydrogen bonds in  $\alpha$ -helices and helix termini in globular proteins, *Proteins: Struct., Funct., Genet.*, 2004, **56**(4), 768–781, DOI: [10.1002/prot.20152](https://doi.org/10.1002/prot.20152).
- 90 E. Bause and G. Legler, The role of the hydroxy amino acid in the triplet sequence Asn-Xaa-Thr(Ser) for the N-glycosylation step during glycoprotein biosynthesis, *Biochem. J.*, 1981, **195**(3), 639–644, DOI: [10.1042/bj1950639](https://doi.org/10.1042/bj1950639).
- 91 K. R. Phipps and H. Li, Protein-RNA contacts at crystal packing surfaces, *Proteins: Struct., Funct., Genet.*, 2007, **67**(1), 121–127, DOI: [10.1002/prot.21230](https://doi.org/10.1002/prot.21230).

